Neural mechanism of orientation process from visually occluded action in human visual cortex

by

Thanaphop THREETHIPTHIKOON

Student ID Number: 1238003

A dissertation submitted to the
Engineering Course, Department of Engineering,
Graduate School of Engineering,
Kochi University of Technology,
Kochi, Japan

in partial fulfillment of the requirements for the degree of
Doctor of Engineering

Assessment Committee:
Supervisor: Hiroaki Shigemasu
Co-Supervisor: Hiroshi Kadota
Co-Supervisor: Kiyoshi Nakahara
Keizo Shinomori
Yukinobu Hoshino

March 2024

Abstract

Neural mechanism of orientation process from visually occluded action in human visual cortex

Thanaphop THREETHIPTHIKOON
Doctoral Program of Engineering Course, Department of Engineering
Graduate School of Engineering

Orientation processing in humans plays a crucial role in manipulating objects in daily life. Numerous studies have investigated the neural mechanisms underlying orientation processing, spanning from early visual areas to more action-related regions. These studies have highlighted the significance of orientation information in action-related process, as it provides essential spatial cues for successful task performance, particularly when actions are guided by real-time visual feedback. However, how the orientation information is processed during the visually occluded action towards an object remains unclear. To investigate this process, we used functional magnetic resonance imaging (fMRI) techniques to record blood-oxygenation-level-dependent (BOLD) signals during occluded action tasks. The multivariate pattern analysis (MVPA) was used to examine the cortical patterns of BOLD signals associated with orientation processing during occluded grasp. The classification of cortical patterns using MVPA was performed on the selected regions of interest (ROIs). The classification result from ROI was defined as the decoded orientation representation of that area. Additionally, we utilized transfer-type classification or cross-decoding methods to identify shared orientation cortical patterns across conditions. The study focused on two primary research directions in orientation processing. Firstly, we aimed to understand the influence of different types of visually occluded grasping actions on the orientation process. Secondly, we investigated the role of non-visual sensory information and action-related processes in grasping tasks without online visual feedback.

The first research approach examined the influence of visually occluded actions on orientation processing in the visual areas of the brain. Participants were engaged in tasks that involved observing an object and performing a grasping action while their visual input of the object was occluded. The object presented in the experiment had four different orientations. Participants were instructed to perform either a precision grasp, which involved using two fingers and a thumb to hold the object with precision (e.g., holding a pen or pencil), or a

coarse grasp, which required using all five fingers to firmly hold the object. The BOLD signal was recorded during both the visual observation phase and the occluded action phase to investigate the representation of orientation information in the visual areas. The aim was to identify the specific visual cortices that encode orientation in different types of grasping actions and to reveal a generalized representation of the orientation process. MVPA classification was utilized to decode orientation information from selected ROIs within the visual cortices. The same-type classification was applied to determine the ROI that represents the orientation in each grasping type. Transfer-type classification was performed to identify a generalized representation of orientation that is independent of specific grasping types. This approach involved training the classifier using data from one grasping type, such as precision grasp, and then testing it on the data from another grasping type, such as coarse grasp and vice versa. By applying the trained classifier to different grasping types, we aimed to uncover a shared representation of orientation that transcends specific action contexts. The results demonstrated that orientation information can be decoded in early visual areas during visually occluded actions, specifically in area V3d for both coarse and precision grasps. Moreover, the results indicated that orientation can only be decoded from coarse grasping in V1 and V2. Transfer classification analysis revealed that the generalized representation of orientation in V3d is significant during visual observation but not during occluded action. This suggested that the processing of orientation information in early visual areas may differ depending on the action context. Overall, the study provides evidence of a representation of vision-related orientation in V1 and V2 and action-related orientation in V3d, with high classification accuracy for each action type. The results suggest that action-related orientation information may rely on proprioceptive information and/or feedback signals from higher motor areas, depending on the type of action.

The second approach of this study investigated the mechanisms underlying orientation processing in the visual cortices, considering the influence of non-visual sensory input and action-related process. Specifically, we examined the role of tactile and proprioceptive sensations as non-visual sensory inputs, as well as the impact of planned and unplanned grasping processes on orientation representation as the action related process. In this study, we examined BOLD signals in four distinct action conditions: direct grasp, air grasp, non-grasp, and uninformed grasp. Participants were presented with images of a cylindrical object, each having one of two orientations. They subsequently performed one of the four conditions and later judged the orientation across all conditions. Notably, all grasping actions

were executed without real-time visual feedback, enabling us to investigate the contribution of tactile input, proprioceptive input, and action-related processes to the processing of orientation information. MVPA was used to examine the differences in cortical patterns among the four action conditions. In addition, transfer-type classification, also known as cross-decoding, was performed to identify shared patterns across action conditions related to the orientation process. Significance in the transfer classification results suggests the presence of a generalized representation within an area, encompassing either input sensory-related or output action-related information. The results demonstrated significant decoding accuracy above chance level for direct grasp in most areas. During air grasp, only early visual areas showed significant accuracy, suggesting that tactile feedback from the object influences orientation processing in higher visual areas while the early areas utilized visual information of object that previously observed. The non-grasp condition showed no statistical significance in any area, indicating that without the grasping action, visual information does not contribute to cortical pattern representation. Interestingly, only the dorsal and ventral divisions of the third visual area (V3d and V3v) exhibited significant decoding accuracy during uninformed grasp, despite the absence of visual instructions. This suggests that the orientation representation in V3d is derived from action-related processes, while V3v is involved in the visual recognition process of object visualization. The processing of orientation information during non-visually guided grasping relies on non-visual sources and is specifically divided based on the purpose of action or recognition.

In summary, this doctoral dissertation provides a comprehensive investigation into the processing of orientation information in the human visual cortex during visually occluded actions. The combination of the two research topics sheds light on the neural mechanisms underlying orientation processing in the absence of visual input. The findings contribute to the field by revealing the role of early visual areas in decoding orientation during visually occluded actions, as well as the influence of non-visual sources on orientation representation in higher visual areas. The study highlights the importance of proprioceptive information, tactile feedback, and action-related processes in the processing of orientation information during grasping actions. These insights deepen our understanding of how the human brain integrates non-visual sensory input and feedback from motor system during orientation processing, thereby facilitating action planning and execution.

Keywords: orientation, visually occluded, fMRI, MVPA, action, tactile, proprioception

Table of Contents

List of tables

List of Figures

CHAPTER 1

Introduction

1.1 Structure of this Dissertation

CHAPTER 1 Motivation, Literature Review, and Objectives

CHAPTER 2 Topic 1: Orientation representation of visually occluded action in human visual cortices

- **2.1 Abstract**
- **2.2 Introduction**
- **2.3 Methodology**
- **2.4 Data Analysis**
- **2.5 Results**
- **2.6 Discussion**
- **2.7 References**

CHAPTER 3 Topic 2: Orientation Representation in Human Visual Cortices: Contributions of Non-Visual Information and Action-Related Process

- **3.1 Abstract**
- **3.2 Introduction**
- **3.3 Methodology**
- **3.4 Data Analysis**
- **3.5 Results**
- **3.6 Discussion**
- **3.7 References**

CHAPTER 4 Conclusions

1.2 Motivation and Literature review

Visual information plays a crucial role in perceiving and interacting with objects. Within the realm of visual perception, the processing of object orientation is particularly essential for planning and executing appropriate actions. Previous research has highlighted the involvement of distinct neural pathways in vision for recognition (ventral stream) and vision for action (dorsal stream) (Mishkin et al., 1982; Goodale and Milner, 1992). Notably, orientation processing has been associated with vision for action, as evidenced by the sensitivity of dorsal stream areas to orientation changes during functional magnetic resonance imaging (fMRI) studies (Valyear et al., 2006; Rice et al., 2007).

During visually guided actions toward graspable objects, the intraparietal sulcus (IPS) region within the dorsal stream has been found to exhibit blood-oxygen-level-dependent (BOLD) signal activation (Binkofski et al., 1998; Culham et al., 2003; Cavina-Pratesi et al., 2007). Furthermore, studies investigating hand posture during grasping have shown activation in the posterior intraparietal sulcus, indicating the role of wrist orientation in object manipulation (Faillenot et al., 1997; Monaco et al., 2011). These findings suggest that the dorsal stream, including the IPS region, is crucial for integrating orientation information and preparing appropriate hand gestures for object manipulation.

Interestingly, the influence of grasping actions extends beyond the dorsal stream, as evidenced by the feedback signal from the motor system to the early visual areas during action planning and execution (Petro et al., 2014). This feedback mechanism enhances orientation perception, even when the planned action is later withheld (Gutteling et al., 2011, 2013, 2015). It is worth noting that these action-related processes in the early visual cortex are not solely reliant on online visual guidance, as reactivation of BOLD signals has been observed during delayed grasping actions without visual information (Singhal et al., 2013). Additionally, grasping objects in a completely dark environment has shown activation in the V3d area, indicating the persistent involvement of visual processing even in the absence of online visual input (Kilintari et al., 2011).

While previous studies have shed light on orientation processing during visually guided grasping actions and in dark environments, an exploration of these processes in human visual

cortices during visually occluded or blinded grasping actions is still lacking. This gap in knowledge prompted the initiation of the first research topic, "Orientation representation of visually occluded action in human visual cortices." The aim was to investigate the orientation process during visually occluded grasping actions and examine how the absence of online visual guidance impacts the neural mechanisms underlying orientation processing.

Without online visual guidance, grasping engages a complex interplay of multiple processes that rely on visual information to perceive object orientation. Tactile and proprioceptive sensations serve as essential sensory input information, while action-related processes encompass planning and execution, serving as feedback signals from motor system. Understanding how orientation processing is influenced by these non-visual sensory inputs and action-related process can provide valuable insights into the intricate mechanisms underlying human vision and action.

Building upon these findings, the second research topic, "Orientation Representation in Human Visual Cortices: Contributions of Non-Visual Information and Action-Related Processes," aims to further investigate the role of non-visual information and action-related processes in orientation representation. By delving deeper into the neural mechanisms involved in orientation processing and considering the contributions of tactile, proprioceptive, and action-related processes, this doctoral dissertation endeavors to bridge the existing gaps in our understanding.

To achieve this, functional magnetic resonance imaging (fMRI) combined with multivariate pattern analysis (MVPA) will be employed to decode blood-oxygenation-level-dependent (BOLD) signals. Real three-dimensional (3D) objects at various orientations will serve as stimuli, enabling the examination of specific orientation pairings for classification in both 2D and 3D orientations. Two types of grasping actions, reflecting different hand gestures, will be performed during the occluded action phase to explore the effects of gesture on orientation processing. The classification of orientation will be divided into same-type and transfer-type categories, elucidating brain regions that specifically represent orientation for each action type and identifying areas with a generalized representation of orientation across different action conditions.

Based on previous research, high decoding accuracy is expected in the early visual areas and the dorsal division of the third visual area (V3d) during instructed grasping conditions,

highlighting the influence of planned actions on the orientation process (Gutteling et al., 2015; Kilintari et al., 2011). Moreover, cross-decoding analyses will shed light on shared patterns of orientation representation between grasping actions with and without instruction, providing insights into the integration of non-visual sensory inputs and action-related processes within the dorsal visual pathway areas (Culham et al., 2003; Singhal et al., 2013).

By investigating the role of non-visual sensory inputs and action-related processes in orientation processing during visually occluded grasping actions, this doctoral dissertation aims to contribute to our understanding of the complex interplay between human vision and action. The findings may have implications for fields such as neurorehabilitation, prosthetics, and robotics, where the integration of sensory information and action planning is crucial for successful interactions with the environment.

1.3 Objectives

Topic 1: Orientation representation of visually occluded action in human visual cortices

- To investigate the orientation representation from visual observation and visually occluded actions in the human visual cortices. We used two grasping types with four different object orientations. We hypothesized that orientation can be decoded from early visual areas, and IPS areas, by a feedback signal from the motor system along with the preparation from the observation phase. The areas V3d and IPS were candidates for the generalized orientation representation from the involvement of grasping action both blindly and visually guided.

Topic 2: Orientation Representation in Human Visual Cortices: Contributions of Non-Visual Information and Action-Related Process

- To investigate how orientation representation is affected by input information from the non-visual sensory system and from action-related processes. The non-visual sensory system refers to the tactile and proprioceptive sensation. The action-related process refers to the action planning process and action execution.
- To find that whether the orientation can be perceived without the visual information but relied on non-visual information in visual cortices.

1.4 Reference in CHAPTER 1

1. Mishkin, M., Ungerleider, L. G., & Macko, K. A. (1983). Object vision and spatial vision: two cortical pathways. Trends in Neurosciences, 6, 414–417. https://doi.org/10.1016/0166-2236(83)90190-x
2. Goodale, M. A., & Milner, A. (1992). Separate visual pathways for perception and action. Trends in Neurosciences, 15(1), 20–25. https://doi.org/10.1016/0166-2236(92)90344-8
3. Valyear, K. F., Culham, J. C., Sharif, N., Westwood, D., & Goodale, M. A. (2006). A double dissociation between sensitivity to changes in object identity and object orientation in the ventral and dorsal visual streams: A human fMRI study. Neuropsychologia, 44(2), 218–228. https://doi.org/10.1016/j.neuropsychologia.2005.05.004
4. Rice, N. J., Valyear, K. F., Goodale, M. A., Milner, A. D., & Culham, J. C. (2007). Orientation sensitivity to graspable objects: An fMRI adaptation study. NeuroImage, 36, T87–T93. https://doi.org/10.1016/j.neuroimage.2007.03.032
5. Binkofski, F., Dohle, C., Posse, S., Stephan, K. M., Hefter, H., Seitz, R. J., & Freund, H. J. (1998). Human anterior intraparietal area subserves prehension: A combined lesion and functional MRI activation study. Neurology, 50(5), 1253–1259. https://doi.org/10.1212/wnl.50.5.1253
6. Culham, J. C., Danckert, S. L., Souza, J. F. X. D., Gati, J. S., Menon, R. S., & Goodale, M. A. (2003). Visually guided grasping produces fMRI activation in dorsal but not ventral stream brain areas. Experimental Brain Research, 153(2), 180–189. https://doi.org/10.1007/s00221-003-1591-5
7. Cavina-Pratesi, C., Goodale, M. A., & Culham, J. C. (2007). FMRI Reveals a Dissociation between Grasping and Perceiving the Size of Real 3D Objects. PLoS ONE, 2(5), e424. https://doi.org/10.1371/journal.pone.0000424
8. Faillenot, I. (1997). Visual pathways for object-oriented action and object recognition: functional anatomy with PET. Cerebral Cortex, 7(1), 77–85. https://doi.org/10.1093/cercor/7.1.77
9. Monaco, S., Cavina-Pratesi, C., Sedda, A., Fattori, P., Galletti, C., & Culham, J. C. (2011). Functional magnetic resonance adaptation reveals the involvement of the dorsomedial stream in hand orientation for grasping. Journal of Neurophysiology,

106(5), 2248–2263. https://doi.org/10.1152/jn.01069.2010

10. Petro, L. S., Vizioli, L., & Muckli, L. (2014). Contributions of cortical feedback to sensory processing in primary visual cortex. Frontiers in Psychology, 5. https://doi.org/10.3389/fpsyg.2014.01223
11. Gutteling, T. P., Kenemans, J. L., & Neggers, S. F. W. (2011). Grasping Preparation Enhances Orientation Change Detection. PLoS ONE, 6(3), e17675. https://doi.org/10.1371/journal.pone.0017675
12. Gutteling, T. P., Park, S. Y., Kenemans, J. L., & Neggers, S. F. W. (2013). TMS of the anterior intraparietal area selectively modulates orientation change detection during action preparation. Journal of Neurophysiology, 110(1), 33–41. https://doi.org/10.1152/jn.00622.2012
13. Gutteling, T. P., Petridou, N., Dumoulin, S. O., Harvey, B. M., Aarnoutse, E. J., Kenemans, J. L., & Neggers, S. F. (2015). Action Preparation Shapes Processing in Early Visual Cortex. The Journal of Neuroscience, 35(16), 6472–6480. https://doi.org/10.1523/jneurosci.1358-14.2015
14. Kilintari, M., Raos, V., & Savaki, H. E. (2011). Grasping in the Dark Activates Early Visual Cortices. Cerebral Cortex, 21(4), 949–963. https://doi.org/10.1093/cercor/bhq175
15. Singhal, A., Monaco, S., Kaufman, L. D., & Culham, J. C. (2013). Human fMRI Reveals That Delayed Action Re-Recruits Visual Perception. PLoS ONE, 8(9), e73629. https://doi.org/10.1371/journal.pone.0073629

CHAPTER 2

Topic 1: Orientation representation of visually occluded action in human visual cortices

2.1 Abstract

Object orientation is crucial visual data for human action planning and execution. Prior research highlights the profound association of orientation with action in visual cortices during the visually guided action. However, how orientation process is represented during visually occluded various actions remains unclear. To investigate this condition, we recorded blood-oxygenation-level-dependent (BOLD) signals while participants performed a visual observation (vision phase) and occluded action (action phase) task using an object shown in four different orientations with +45°/−45° rotation around the roll and pitch axes. The occluded action tasks comprised full and precise grasps. Our experiment aimed to investigate orientation representation of each action type and uncover a generalized representation of orientation in visual areas. We employed multivariate pattern analysis (MVPA) on functional magnetic resonance imaging data to classify orientation representation in specific visual cortices. Results indicated that orientation information is decodable in early visual areas during occluded actions, particularly in V3d for both grasp types, whereas V1 and V2 show decoding only for full grasping. Transfer classification, assessing a generalized representation of orientation irrespective of action types, revealed significant results in V1, V2, and V3d during visual observation, but during occluded action found significance only in V1 and V2. In summary, our findings highlight a representation of vision-related orientation in V1 and V2, and action-related orientation in V3d. Specifically, V3d shows an action-specific process aiding the orientation process in via cortical pattern. This implies that action-related orientation information may be dependent on the type of action performed.

2.2 Introduction

Visual information is crucial for perceiving object features, with orientation playing an essential role in planning subsequent actions, guiding appropriate hand gestures for grasping. Visual information traverses two pathways beyond the early visual cortex (EVC) for recognition (ventral stream) and action (dorsal stream) (Mishkin et al., 1983; Goodale & Milner, 1992). Subsequent evidence, particularly from functional magnetic resonance imaging (fMRI) studies, highlights the dorsal stream's sensitivity to orientation changes, especially when interacting with graspable objects (Valyear et al., 2006; Rice et al., 2007) When grasping real objects, activation of blood-oxygen-level-dependent (BOLD) signals occurs in the intraparietal sulcus (IPS) of the dorsal stream, as noted in studies on visually guided actions (Binkofski et al., 1998; Culham et al., 2003; Cavina-Pratesi, Goodale, & Culham, 2007). In addition, varied wrist orientations during grasping elicit activation in the posterior intraparietal sulcus (Faillenot et al., 1997; Monaco et al., 2011). In later study, the signal of the action-related process is fed back to the early visual area when planning through executing the action (Petro, Vizioli & Muckli, 2014). Feedback from action-related processes to the early visual area enhances orientation perception during grasping, even when the action is withheld (Gutteling, Kenemans, & Neggers, 2011; Gutteling et al., 2013, 2015), indicating the presence of action-related content in the EVC and dorsal stream.

Conversely, when vision is unavailable for action execution, the EVC shows reactivation of BOLD signals when performing a delayed grasping action onto an object even without online visual information (Singhal et al., 2013), supporting action-related feedback signal studies. Concurrently, grasping an object in a completely dark environment after visual observation showed activation in the monkey V3d area using the quantitative 14C-deoxyglucose method (Raos & Savaki, 2010; Kilintari et al., 2011). Additionally, the haptic information from blinded exploration is processed in parietal areas and early visual areas (Marangon, Kubiak, & Króliczak, 2016; Monaco et al., 2017) suggesting that without online visual guidance, action-related content still existed in the EVC.

To date, the exploration of orientation processing in the human visual cortex during diverse grasping actions in visually occluded tasks is limited in the existing literature. The previous study investigated the orientation representations, tactile sensory input, action processing for different grasping conditions. The recent study revealed optimal accuracy when there was visual information and tactile feedback from an object (Threethipthikoon et al., 2023).

However, the investigation used only one type of action (whole hand grasp); thus, it is unclear whether the study decoded only the action representation and not the object orientation. To address this, our current study aims to investigate orientation processing during visual observation (vision phase) and visually occluded action (action phase) involving different action types. We used fMRI to analyze BOLD signals with the multivariate pattern analysis (MVPA) classification method, which can decode the difference between conditions that the univariate method results in similar activation level. The classification method was used to determine the orientation representation of the cortical pattern. Using a real three-dimensional (3D) object at four orientations as stimuli, presented during the vision phase, allowed us to explore multiple orientations. The object, possessing an elongated cylindrical form, aligns with the grasping processes of the dorsal and ventral visual streams (Fabbri et al., 2016). In the occluded action phase, two types of grasping actions were performed to examine the impact of different gestures on orientation processing, considering the involvement of vision for action (Binkofski et al., 1998; Culham et al., 2003). If the representation is generalized, the decoded orientation during occluded action should not be action-dependent but relevant to the object's orientation. We categorized orientation classification into same-type and transfer-type, based on the data type in classifier training and testing. The same-type classification identified brain areas specifically representing orientation for each action type, with high classification accuracy expected in EVC areas and the dorsal stream during the vision phase. In the action phase, our hypothesis proposes that orientation can be decoded from V1, V2, V3d, and IPS areas, aided by a feedback signal from the motor system and preparation from vision phase instructions. Distinct decoding results for each action type are anticipated in action-related areas. Furthermore, transfer-type classification aims to identify areas with a generalized orientation representation, independent of the action, by training and testing on different grasping types. V1, V2, V3d, and IPS emerge as candidates for generalized orientation representation, supported by evidence of their involvement in both visually guided and blindly executed grasping actions (Raos & Savaki, 2010; Kilintari et al., 2011; Singhal et al., 2013).

2.3 Methodology

2.3.1 Participants

Ten human participants (four females, six males; age mean ± SD, 23 ± 4.2) were recruited from a location which will be identified if the article is published for the fMRI experiments. They had normal or corrected-to-normal vision and all of them were right-handed. All participants were paid for their participation in this research. Regarding their medical background, no participants reported any mental illness or neurological disease. This study and its protocol were approved by the Human Research Ethics Committee of Kochi University of Technology (138-C2) after all participants provided written informed consent according to the Declaration of Helsinki.

2.3.2 Experimental Design

Experiments were conducted to investigate the cortical representation of object orientation obtained from grasping actions in a visually occluded environment. Four orientation angles and two types of grasps were used with a 3D object as the stimulus (Figure 2.1A, B). In different conditions, this was presented in orientation angles of 45° or −45° on the roll and pitch axes, producing four orientation conditions (Figure 2.1A). The two types of grasping action were full and precise grasps (Figure 2.1B). The full grasp involved using all five fingers to firmly hold the object, while the precise grasp was defined using only two fingers and a thumb to hold an object that requires precise usage (e.g., holding a pen or pencil). The purpose of using two grasping types was to see the effect of the different grasping gestures in the decoded representation and whether the grasping types affect the orientation processing or not.

The experimental design comprised of two sessions: a control session and a grasping session (Figure 2.1C, D). The control session required participants to observe and judge the object's orientation whereas the grasping session required participants to perform a grasping action on the occluded object following its initial observation. The purpose of the control session was to examine orientation processing that used only the orientation information from an object. Therefore, this session excluded the grasping instructions given in the other sessions. The judgments of the observed orientation of an object were also recorded. In the grasping session,

we aimed to determine whether the type of grasp affected the representation of the occluded object. We hoped this data would provide an orientation processing representation for each action type and the orientation representations common to both action types.

In the control session (Figure 2.1C), the flap cover opened to show the object for 2 s at the beginning of each trial, followed by a fixation period for 8 s with the closed flap until the next trial. The participants were instructed to recognize the object orientation in this vision phase. Thereafter, the participants pressed the keypad answering the corresponding orientation in the judgment phase for 2 s, followed by a fixation period for 8 s. Keypad answers were either the "near" or "far" and "left" or "right" buttons depending on the previously observed orientation.

In the grasping session (Figure 2.1D), the vision phase was similar to that of the control session but with the addition of an instruction buzzer for the grasping type in the next phase. The buzzer had two different pitch sounds: high pitch for the precise grasp and low pitch for the full grasp. Then, as an action phase, the participant grasped the visually occluded object as instructed within a 2 s period, followed by a 10 s fixation period. The period with grasping action may cause longer hemodynamic delay signal sustaining than the button pressing period in the control session due to the large movement time.

Each experimental session comprised 10 runs and each experimental run included 16 trials with different combinations of the orientations and grasp types. The control sessions each had four conditions corresponding to the four orientations with four repetitions, while the grasping sessions each had eight conditions with two repetitions (2 action types × 4 orientations × 2 repetitions). The conditions were presented randomly using an event-related design paradigm. The trials were repeated 20 times for each condition. Each participant performed 160 trials.

The answers from all judgment tasks per run were recorded to calculate the orientation perception performance of each subject. Tasks without any answers were not included in the calculation. All participants were required to keep their head still and look at the fixation cross in the center of the flap cover. Any runs with extravagant head movement were discarded. Extravagant head movement was defined as a head movement >2 mm and/or head rotation >2° from the first scan in each run. All participants could maintain still during ≥8 echo-planar imaging (EPI) runs.

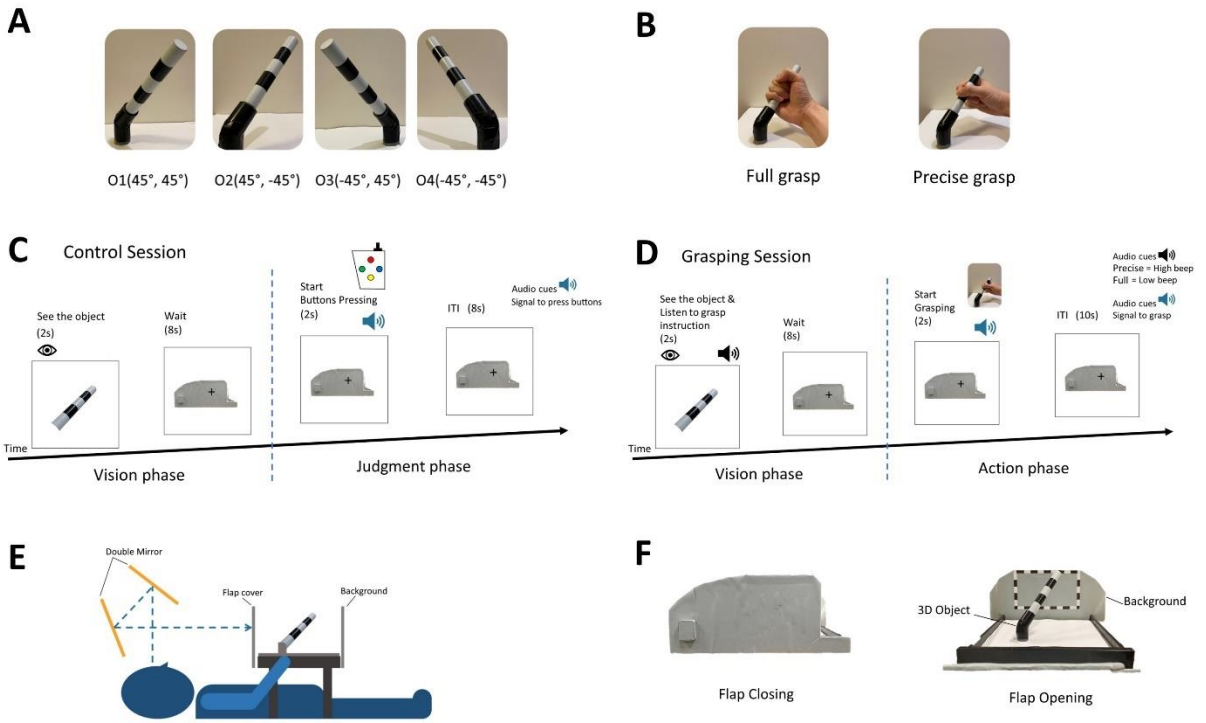

Figure 2.1 (A) Illustration of the object in four orientations. The object rotates in roll and pitch axes of 45° and −45° as follows: O1 (45°, 45°), O2 (45°, −45°), O3 (−45°, 45°), and O4 (−45°, −45°). The rotated angle in the roll axis represents the 2D orientation difference. The rotated angle in the pitch axis represents the 3D orientation difference. (B) Illustration of the two grasping types: full and precise. (C) Experimental diagram displaying the trial in the control session. (D) Experimental diagram displaying the trial in the grasping session. (E) Experimental setup: the participant sees the object through the two-mirror setup located above the head coil for a direct angle presentation of the object in each orientation. (F) Photos of the frame support that was on the MRI-compatible table. The front flap cover has a movable hinge to control the 3D object's visibility by the experimenter. When the flap covers an object, the participant fixes their gaze on the fixation cross. When the flap is opened, the participant sees the object through the mirror in (E) with the frame background.

2.3.3 Stimuli

Participants observed the object through two angled mirrors situated above the head coil (Figure 2.1E). The double mirror setting was applied for the exact object orientation perception in the vision phase. All participants had practiced the action task with visual guidance prior to the experimental session. In the control session, an MRI-compatible keypad was used to collect the orientation judgment data from the participant and participants had practice answering the judgment prior to the start of the session.

The object was placed on the table at the participant's hip area and a wooden frame was used to fix the base of the object (Figure 2.1F). The frame had a lever for the experimenter to

control the flap cover presenting or occluding the object (Figure 2.1F). A gray flap was used to cover the stimuli during the fixation and action phase (Figure 2.1F right). In the vision phase, the uncovered stimuli showed the object over a gray background with a rectangular striped frame (Figure 2.1F left).

The experimental stimulus was a cylindrical object made from plastic with black and white stripes (Figure 2.1F). The object was 12.5 cm by 1.8 cm in length and diameter, and it was presented in four different orientations, rotated in combination of 45° or −45° on the roll and pitch axes as follows: O1 (45°, 45°), O2 (45°, −45°), O3 (−45°, 45°), and O4 (−45°, −45°) (Figure 2.1A).

2.3.4 fMRI Data Acquisition

All scanned images were acquired using a 3 Tesla Siemens MAGNETOM Prisma MRI scanner at the Brain Communication Research Center of the Kochi University of Technology. MRI-compatible foam pads were used to fix the participants' heads to reduce movement. A high resolution T1-weighted anatomical scan (1 mm3) was acquired for each participant and regions of interest (ROIs) were localized in all separate sessions. In each experiment run, BOLD signals were measured with an EPI sequence [echo time (TE): 58 ms; repetition time (TR): 2000 ms; number of volumes per run: 182; slice thickness: 3 mm; slice acquisition order: interleaved] for 34 slices covering the visual cortex, posterior parietal cortex, and posterior temporal cortex. For the structural data, a T2-weighted structural image of each participant was retrieved in a 2.5-min run and recorded before the first corresponding EPI data in one session. The T2-weighted structural data were used as reference slices for EPI data motion correction and co-registration between T1-weighted anatomical images and EPI data in native anatomical space. Thereafter, all data were converted to Talairach coordinates for MVPA trial extraction.

Our study aimed to investigate the representation of orientation during visually occluded action covering the early, the higher dorsal, and the ventral visual areas (Figure 2.2A). According to the localizer protocol, each participant's ROI was individually delineated into retinotopically localized early visual areas, V1, V2, V3d, V3v, and V3A, determined using an expanding ring and rotating wedge (Sereno et al., 1995; DeYoe et al., 1996; Warnking et al., 2002). V7 was found to be anterior and dorsal to V3A. In addition, we included the lateral occipital cortex (LOC) from the ventral stream, which shows a higher level of activation for intact images than for scrambled images (Kourtzi and Kanwisher, 2000, 2001). Separate

localizers were used to identify the higher dorsal areas hMT+ and kinetic occipital region (KO), along with the following IPS areas: the ventral intraparietal sulcus (VIPS), parieto-occipital intraparietal sulcus (POIPS), and dorsal intraparietal sulcus (DIPS). hMT+ was defined as an area with a high level of activation in response to inward and outward motion of dots (Zeki et al., 1991) and KO was defined as an area with a high level of activation for motion-defined contours (Dupont et al., 1997; Zeki et al., 2003). Finally, the IPS area was identified by contrasting the activity of 3D shapes generated by rotating motion with that of 2D shapes generated along a frontoparallel plane (Vanduffel et al., 2002). In addition, the anterior intraparietal area of non-human primates has selectivity for shape, size, and orientation of objects during grasping 3D objects (Murata et al., 2000). This area was proposed to be the homologue in human dorsal IPS anterior through multiple functional tests (Orban, 2016). The signal patterns from each ROI were used for creating the classification sample data. Both left and right hemisphere patterns were merged into a representation of each ROI.

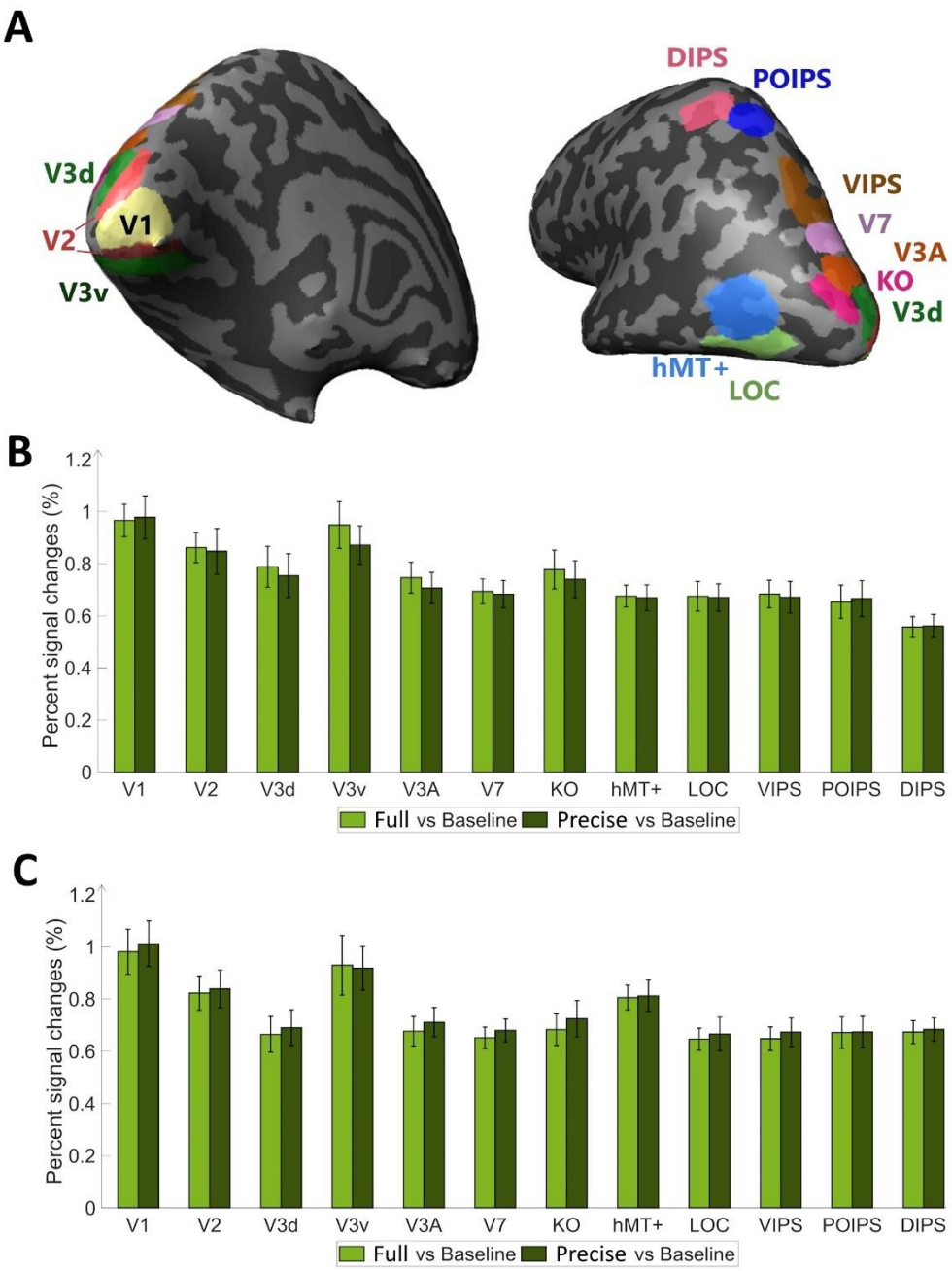

Figure 2.2 Regions of interest (ROI) used in the experiment and percentage of signal changes in the studied areas. (A) The ROIs contain areas in visual cortices. Our study's early visual cortex (EVC) includes the areas V1, V2, V3d, and V3v. The dorsal areas include V3A, KO, hMT+, and V7. The intraparietal sulcus (IPS) areas comprise the ventral intraparietal sulcus (VIPS), parieto-occipital intraparietal sulcus (POIPS), and dorsal intraparietal sulcus (DIPS). The dark gray pattern indicates the sulci, whereas the light gray one indicates the gyri. The ROIs were individually delineated by standard localization sessions (see the fMRI acquisition section). (B) Percent signal changes of the areas in "stimuli versus baseline" condition. (C) Percent signal changes of the areas in "grasping versus baseline" condition. The error bars indicate the standard error of the mean from all participants (n = 10). All areas displayed percent signal changes significantly above the 0 from the t-test in group data (*$p < 0.005$).

2.4 Data Analysis

2.4.1 Pre-Processing

We performed data processing and analysis using the FreeSurfer software package (Fischl, 2012), BrainVoyager 21 (Version 21.0.0.3720, 64-bit; BrainInnovation, Maastricht, Netherlands), and MATLAB R2020b (The MathWorks, Natick, MA, USA). FreeSurfer was used to extract the white matter (WM) and gray matter (GM) from T1-weighted 3D anatomical image. Then, the WM was applied as a segmentation mask with GM in BrainVoyager, and the extracted brain was transformed into the Talairach space for generating the cortical surface. Subsequently, the inflated cortical surface was used to delineate ROIs for MVPA. 3D motion correction was applied to EPI data using the T2-weighted image from the beginning of the session without spatial smoothing. Co-registration of the EPI data with the T1-weighted image was performed, followed by transformation into the Talairach space.

2.4.2 ROI-Based Univariate Analysis

We conducted a univariate analysis of the overall BOLD signal pattern in each selected ROI. The average BOLD signal pattern was defined as the percentage of signal changes in each phase, comparing the task state to the baseline state defined from the initial visual fixation and the end of the run. We predicted high signal changes in the visual areas involved earlier in visual processing, with a decrease in the extent of the signal changes in the higher order areas later along the processing pathway. In addition, we looked for univariant differences between the grasp types (full or precise). The hemodynamic delay of the BOLD signal was calculated as three volumes (6 s). We used the average of the percent signal changes over all runs and all participants for further analysis.

2.4.3 ROI-Based MVPA

MVPA is a well-known analytical approach with great sensitivity in detecting different conditions. We ran MVPA on the EPI data from each ROI. To classify MVPA, a linear support vector machine (SVM) was utilized as a binary-classifier in MATLAB. The

classification was performed using two approaches: same-type and transfer-type classifications (Figure 2.3). In the same-type classification, the same grasping type was used in both training and testing SVM to investigate a cortical pattern specific in orientation of each action type (Figure 2.3A). In contrast, the transfer-type classification used different grasping types for training and testing in SVM, such as training in the full grasping type and then testing in the precise type and vice versa (Figure 2.3B). The results from the transfer classification served to assess the common pattern shared across grasping conditions.

For the classification of each ROI, we used pairings of two distinct orientations in the same depth: O1 vs. O3 and O2 vs. O4 (Figure 2.3A-1 to 2.3A-4). This was considered a 2D orientation classification. Additionally, the 3D orientation classification was later performed on the different depth pairs: O1 vs. O2 and O3 vs. O4 (Figure 2.3A-5 to 2.3A-8). The classification results were averaged together and defined as the orientation classification of that ROI.

Each ROI was selected from both hemispheres and consisted of the top 250 voxels with contrast on stimulus vs. fixation baseline. In participants where there were <250 voxels in the ROI, the total voxels were used. The average value from the two volumes at 6 seconds after the onset was used as the ROI data. The two volumes before the onset time served as the baseline for the cortical pattern. The differences between the ROI data and baseline data were transformed into z-scores and transmitted to SVM for training and testing.

The laterality of the grasping action was investigated by performing a 2D orientation classification separately for each hemisphere. To explore potential lateralization patterns in visually occluded actions and specifically examine whether actions executed with the right hand toward the target showed differential lateralization, the ROI-based MVPA classification was replicated for both, the left and right hemispheres. The analysis followed the same procedure as the standard ROI-based MVPA, but used only half of the ROI data for each hemisphere.

In each classification, the leave-one-run-out method was used to evaluate the MVPA classification performance. The testing data belonged to one run while the rest of the data from other runs were used as the training data. This method was repeated for all runs, and the accuracy of each iteration was averaged to determine the accuracy of each participant. Then, the classification accuracies across participants were averaged for each ROI.

To determine the statistical significance of MVPA, we performed a two-tailed one-sample t-test across participants with chance level of decoding (50%) for each ROI. To ensure the accuracy of significance for each ROI, we applied the false discovery rate method (FDR) to

correct for multiple comparisons (Benjamini and Yekutieli, 2001). Particularly, FDR was applied for all analyses across the 12 ROIs within the same condition, including sessions, phases, and grasping types. A post hoc power analysis was performed for all results with the same principle as FDR. The sample size and calculated effect size were entered into the analysis according to Cohen's d method to determine the statistical power (1 - β err prob) of the decoding results.

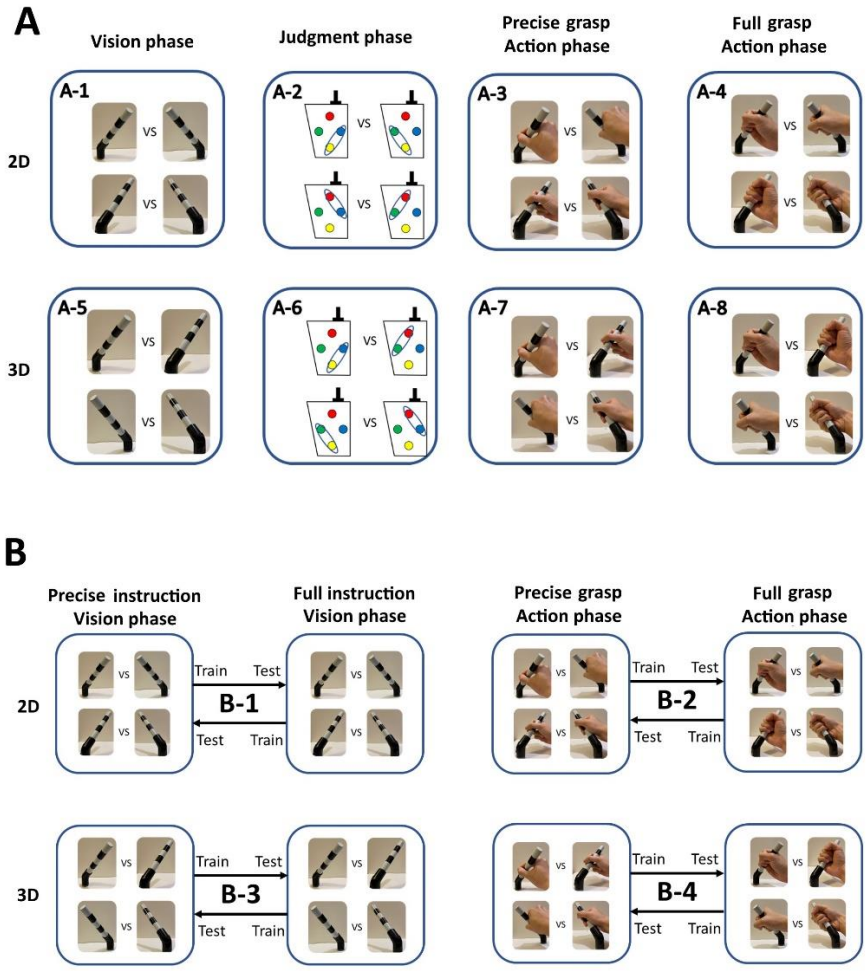

Figure 2.3 Schematic representation of ROI-based MVPA orientation classification in the control session and grasping session. (A) The complete schematics of "same-type classification" are as follows: (A-1) Pairs of 2D orientation classification during the "vision phase" in both sessions. (A-2) Pairs of 2D orientation classification representing the selected buttons pressed during the "judgment phase" of the control session. (A-3 and A-4) Pairs of 2D orientation classification for "precise grasp" and "full grasp" during the "action phase" of the grasping session. (A-5 to A-8) The schematics of the 3D orientation classification pairs are depicted in a manner consistent with the previous four schematics in 2D orientation classification (A-1 to A-4). (B) The complete schematics of "transfer-type classification" are as follows: (B-1) Pairs of transfer-type 2D orientation classification in the "vision phase" of the grasping session. (B-2) Pairs of transfer-type 2D orientation classification in the "action phase" of the grasping session. (B-3 and B-4) Schematics of transfer-type 3D orientation classification pairs depicted in a manner consistent with the previous two schematics.

2.5 Results

2.5.1 ROI-Based Univariate Analysis

The univariate analysis was performed to investigate characteristics of BOLD signal changes level for the vision phase and action in visual areas. Figure 2.2A, 2.2B, and 2.2C shows the ROIs and the average percentage signal changes from each area in all runs of all participants. The results for stimuli vs. baseline (Figure 2.2B) and grasping vs. baseline (Figure 2.2C) showed overall percent signal changes significantly higher than zero ($p < 0.005$). BOLD signals were stronger than the fixation baseline during the stimuli and grasping conditions. The intensity levels of percent signal changes decreased from early to higher visual areas. However, there were no significant differences among the visual and grasping conditions between areas. No statistically significant differences were found between the grasp types, suggesting that cortical activity was detected for each type. Given these univariate results, we used MVPA to acquire further insights into the processing characteristics for each condition.

2.5.2 ROI-Based MVPA Results

2.5.2.1 Control session classification

In this session, participants observed the object and judged its orientation. Orientation classification was performed on the BOLD data from ROIs in visual cortices separated into the vision and judgment phases in the control session. The purpose of this session was to investigate the orientation representation in ROIs decoded from observation alone with no grasping instruction and execution. In the vision phase, the orientation classification was anticipated to be statistically significant above the chance level (50%) corrected by FDR in the EVC. Accordingly, the classification results showed a significantly high accuracy in V1, V2, V3d, V3A, V7, KO, and hMT+ (Figure 2.4A). This was according to the retinotopic related orientation sensitivity with visual stimuli as studied in previous studies. In the judgment phase, the orientation representation was decoded from the button pressing answering the corresponding object orientation observed in the vision phase without direct-action onto the object (Figure 2.3A-2). Overall, the decoding accuracy demonstrated higher than chance level in V2, V3d, V7, and KO (Figure 2.4A). This suggested orientation

representation with no grasping action related pattern but from the task of judgment itself.

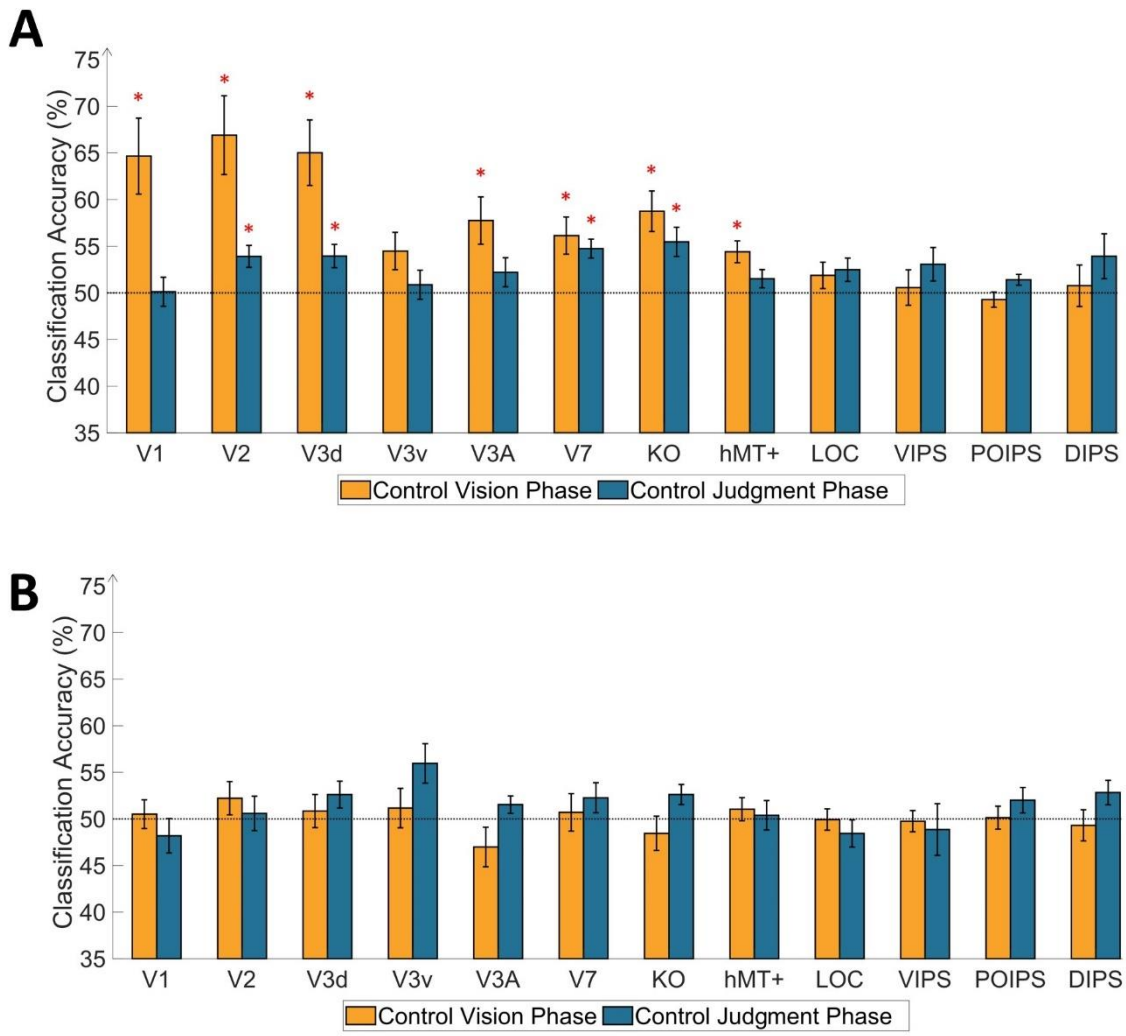

Figure 2.4 Results of ROI-based MVPA orientation classification in the control session in 2D and 3D. (A) The bar graph illustrates 2D orientation classification results in both phases of each area by classification accuracy and areas. (B) The bar graph illustrates 3D orientation classification results in both phases of each area by classification accuracy and areas. The dashed line indicates the chance level of classification at 50%. The error bars depict the standard error of the mean across the participants (n = 10). The red asterisk indicates statistical significance above the chance level (50%) based on two-tailed t-tests across the subjects ($p < 0.05$) and an FDR correction of $q < 0.05$.

2.5.2.2 Same-type classification

The same-type classification defined the orientation difference within the visual areas during observed and grasp an object. In ROI, the significant classification or decoding results mean that the orientation was represented in that area. The analysis was separated into the vision and action phases (Figure 2.3A-1, 2.3A-3, and 2.3A-4). During the vision phase of the

grasping session, different buzzer instructions (high or low pitch) were delivered, but the visual input was the same for both grasping types. Consequently, the accuracies are expected to be comparable among grasping types throughout the vision phase of all sessions.

Early visual areas V2 and V3d exhibited significantly high accuracies for both grasping types, whereas the remaining areas demonstrated decoding accuracy at the chance level, except for V1, which exhibited significantly high accuracy in precise grasp (Figure 2.5A). In contrast, areas V3A, V7, KO, and hMT+ showed lower decoding accuracies than in the control session (Figure 2.4A, 2.5A). In addition, we found no significant differences across grasping types (between precise and full grasping types) in any areas, showing that distinct action instructions had minimal influence on orientation perception when seeing the object.

In the action phase (Figure 2.5B), the full grasping type exhibited higher than chance decoding accuracy in V1, V3d, V3A, VIPS and DIPS. In the same areas, the decoding accuracy demonstrated significantly higher decoding accuracies than in the control session (significance should be added the asterisk in the Figure 2.5B for significance than control session). However, in area V3d, the precise grasp decoding accuracy was only significantly high above chance level and showed difference from the control session. These decoding results suggest the following: First, that areas in the early visual areas and IPS are more involved in the representation of the full grasp action. Second, the precise grasp type may not contribute the orientation-related cortical representations. Third, the V3d area is involved in representations specific to each grasp type. Lastly, the VIPS and DIPS areas had relatively different results between the full and precise grasp conditions (from the uncorrected p).

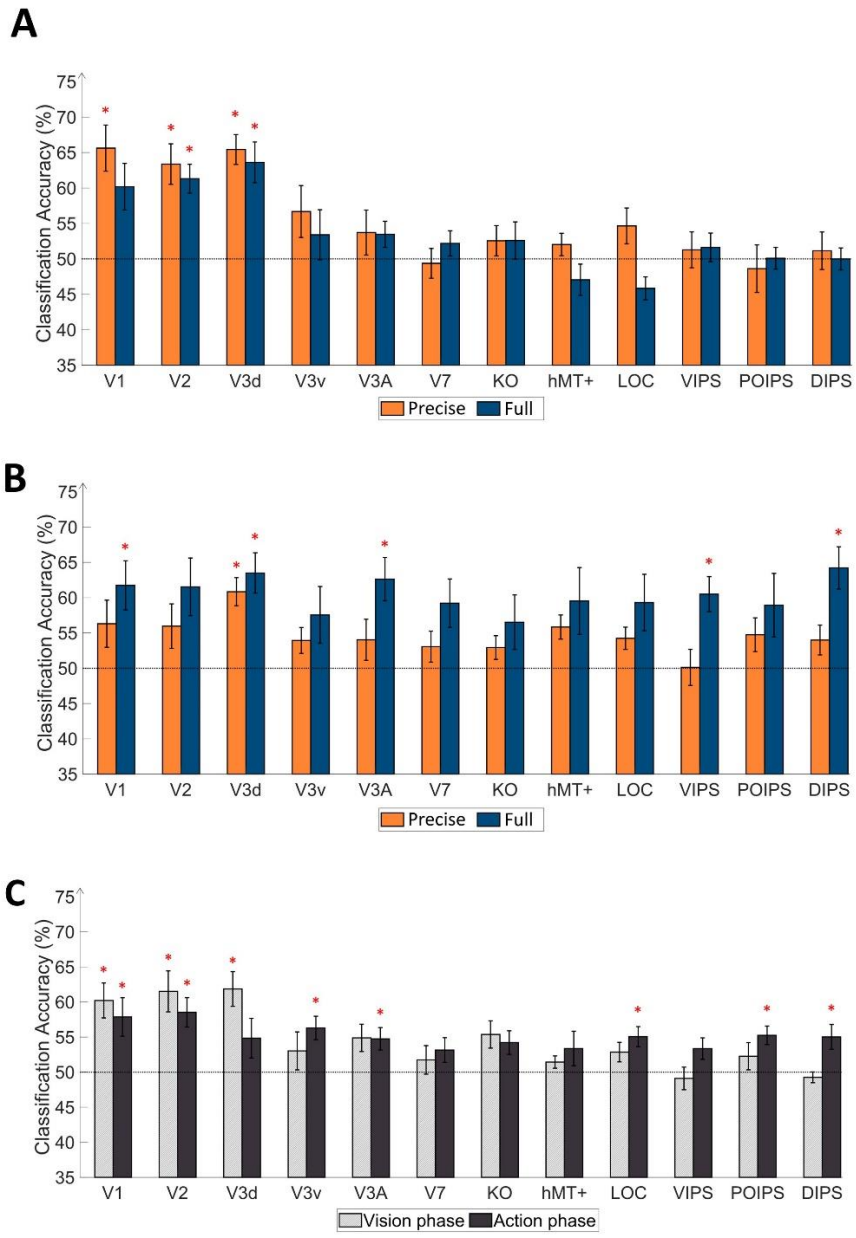

Figure 2.5 Results of ROI-based MVPA orientation classification in the grasping session for 2D orientation. (A) Results of the same-type classification in the vision phase. (B) Results of the same-type classification in the action phase. (C) Results of the transfer-type classification. The bar graph indicates the MVPA classification results for each area, indicating classification accuracy. The dashed line indicates the chance level of classification at 50%. Error bars indicate the standard error of the mean across the participants (n = 10). Red asterisks denote statistical significance above the chance level (50%) based on two-tailed t-tests across the subjects ($p < 0.05$) and an FDR correction of $q < 0.05$.

2.5.2.3 Transfer-type classification

To identify a generalized orientation representation in the vision and action phases, a transfer-type classification or cross-decoding method was performed across grasp types (Figure 2.3B). The significant decoding accuracy in this analysis indicated that ROIs contained an orientation-related cortical pattern common to both action types. Hence, representations of object orientations could be decoded based on these findings. During the vision phase, according to the retinotopic organization, high accuracies were anticipated in early visual areas, but during the action phase, high accuracies were anticipated in V1, V2, V3d, and IPS areas. We expected V1 and V2 to have object-related information common to all orientation representations. We speculate that the cross-decoded representation from V3d might be above the chance level in the action phase as the same-type classification results were significant. At last, the candidates for generalized representation were all IPS areas due to the large amount of action-related content in the dorsal stream (Singhal et al., 2013).

In the vision phase of the transfer-type classification (Figure 2.3B-1), the EVC decoding accuracy was significantly higher than chance (Figure 2.5C). V1, V2, and V3d could classify orientation across the action types. The results here support the hypothesis that the instruction of action may not have an impact on the orientation representation as the cortical pattern can be cross-decoded. In contrast, the cross-decoding results of V3d were only significant in the vision phase, and the action phase showed no significant decoding accuracy. This suggested the unique cortical pattern of each action type in this area.

In the action phase of the transfer-type classification (Figure 2.3B-2), the V3v, V3A, and LOC areas demonstrated significant decoding accuracy. Although the same-type decoding results were significant only for the full grasp type in V3A, there were significant cross-decoding results in all of these areas during the action phase. In some IPS areas, the cross-decoding results showed high decoding accuracies in the action phase of POIPS and DIPS (Figure 2.5C). This result may suggest the influence of the full grasping type since the performance of this grasping type was significant in the same-type decoding. In addition, the DIPS results revealed a relatively high difference between the vision and action phases. DIPS decoding results suggest the impact of different grasping types results in the orientation representation of action phase.

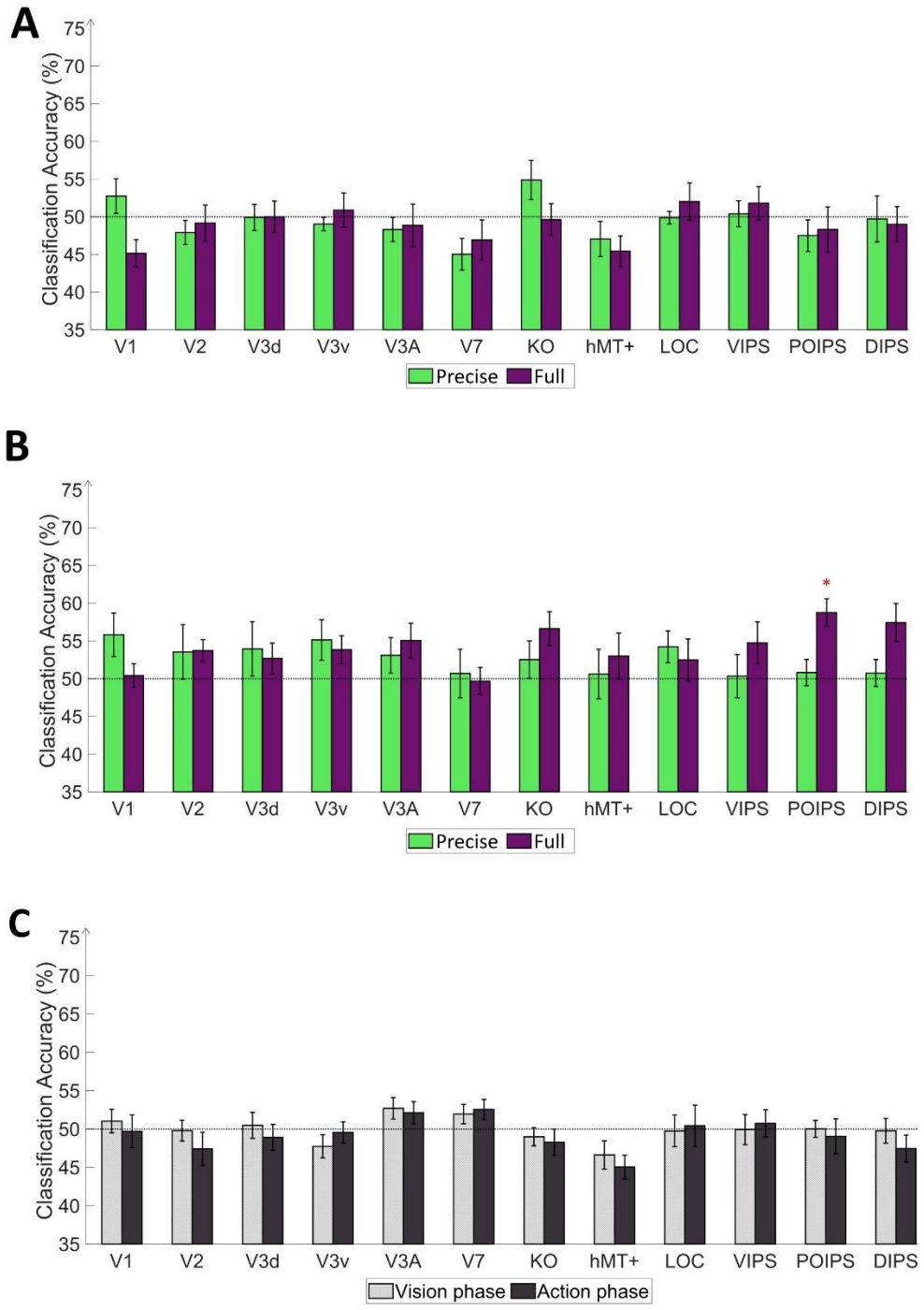

Figure 2.6. Results of ROI-based MVPA orientation classification in the grasping session for 3D orientation. (A) Results from same-type classification in the vision phase. (B) Results from same-type classification in the action phase. (C) Results from transfer-type classification. The bar graph indicates the MVPA classification results for each area, indicating classification accuracy. The dashed line indicates the chance level of classification at 50%. Error bars represent the standard error of the mean across the participants (n = 10). Red asterisks denote statistical significance above the chance level (50%) based on two-tailed t-tests across the subjects ($p < 0.05$) and an FDR correction of $q < 0.05$.

2.5.2.4 3D orientation classification

In addition to the 2D orientation MVPA decoding method, we examined 3D orientation by MVPA using fMRI data from the control and grasping sessions (Figure 2.3A-5 to 2.3A-8). Pairs of different orientations in the pitch axis were defined as 3D orientation differences. This analysis was performed to determine whether the action itself could induce cortical pattern differences based on depth-based alterations in object orientation. Significant decoding results would suggest that a given area contains an orientation representation that incorporates depth differences. The results from the control session showed decoding accuracies around chance level (50%) in the control vision and control judgment phases (Figure 2.4B). In the grasping session, the same-type classification showed decoding accuracies around chance level in the vision phase (Figure 2.6A); however, in the action phase, the decoding accuracy was significantly above the chance level in the POIPS of the full grasping type (Figure 2.6B). This area may suggest 3D orientation representation from the action. Last, the transfer-type classification showed non-significant decoding accuracies around chance level (50%) in all areas (Figure 2.6C). This suggests that, when compared to the 2D orientation, the 3D orientation decoding results showed lower accuracy overall and failed to past the significant criteria in same procedure to the 2D orientation decoding.

2.5.2.5 Laterality Analysis

MVPA was performed for each hemisphere to explore laterality in visually occluded grasping actions. The different pairs of 2D orientation classifications were examined in each hemisphere (Figure 2.3B-1, 2.3B-2). This analysis was performed to investigate the cortical pattern of separate hemispheres in the decoding of 2D orientation representation. In the vision phase, V1, V2, V3d, and V3v of the left hemisphere showed significantly high decoding accuracy in terms of precise grasping (Figure 2.7A-1). V3d showed significantly high decoding accuracy in both hemispheres (Figure 2.7A-2). In the action phase, the left hemisphere V2, V3d, V3A, VIPS, and DIPS areas showed significantly high decoding accuracy in terms of the full grasping type (Figure 2.7B-1). Most right hemisphere areas showed significantly high decoding accuracy in terms of the full grasping type. V2 and VIPS showed a significant difference between the grasping types (Figure 2.7B-2). Lastly, the decoding results of all ROIs indicated no significant differences between the two hemispheres. From the decoding results of this analysis, there were two main findings. First, in half of the

data used in MVPA, significant results in the visual phase occurred primarily in the left hemisphere, while those in the action phase were predominantly in the right hemisphere. Second, the difference between the grasp types found in V2 and VIPS suggests the possibility of distinct cortical patterns for different action types (additional details results are provided in the supplementary document).

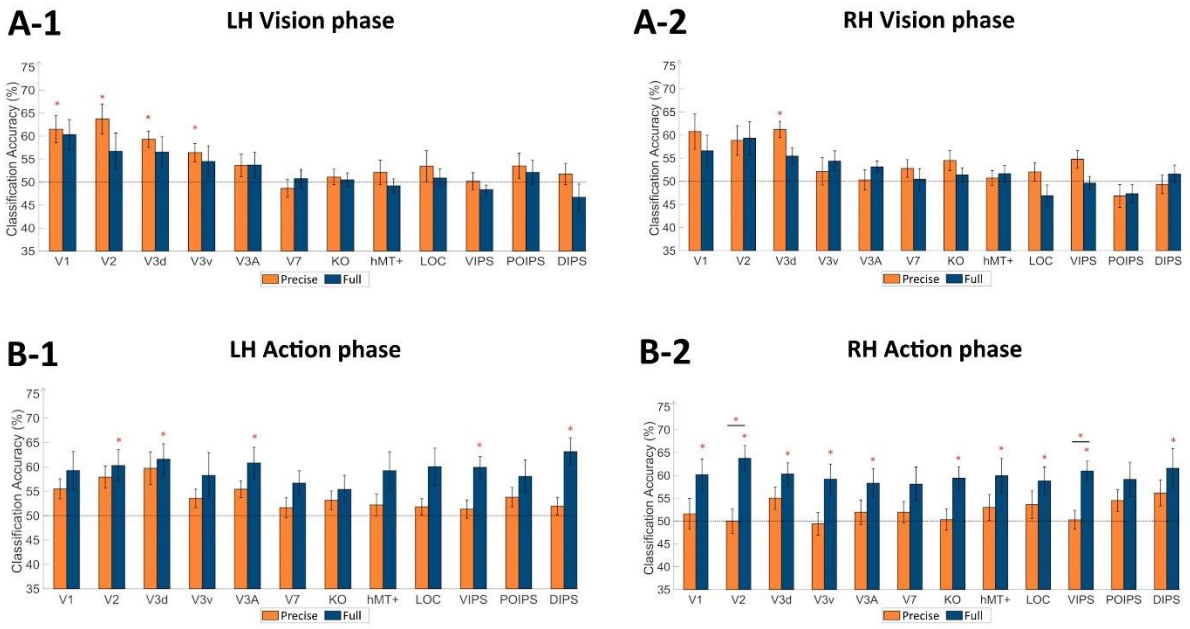

Figure 2.7 The laterality analysis results using ROI-based MVPA orientation classification in the grasping session for 2D orientation. (A) Results from same-type classification in the vision phase. (B) Results from same-type classification in the action phase. The bar graph presents the MVPA classification results for each area, indicating classification accuracy. The dashed line indicates the chance level of classification at 50%. Error bars indicate the standard error of the mean across the participants (n = 10). Red asterisks denote statistical significance above the chance level (50%) or significance difference between two grasping types. The significance was based on two-tailed t-tests across the subjects ($p < 0.05$) and an FDR correction of $q < 0.05$.

2.6 Discussion

This study investigated the representation of orientation during different visually occluded action types by using the MVPA method. In our study, the orientation representations during the occluded action were investigated by applying the MVPA classification method on fMRI data. The overall results from the “same-type classification” showed that orientation can be

decoded in the action phase from the V1, V3d, V3A, and IPS regions regardless of online visual guidance (Figure 2.5B). In particular, V3d demonstrated substantial orientation decoding performance for both grasping types. The higher order dorsal areas, VIPS, and DIPS, showed the significant decoding performance in full grasping types and these areas showed relatively different decoding results between full and precise grasp conditions.

Furthermore, the generalized representation was decoded from V1 and V2 regions suggesting the orientation from the retinotopic organization regardless of the action types (Figure 2.5C). V3d showed significant cross-decoding accuracy in the vision phase but failed to pass the significant criteria in the action phase (Figure 2.5C). This suggested that the orientation representation of each grasping type in the V3d was not transferred in the action phase but implied that V3d processed orientation differently depending on the action type. In IPS areas, the high cross-decoding accuracies in the action phase revealed that the processing of orientation may depend on full grasping type, which suggests the involvement of feedback signals from motor-related areas.

Additionally, the 3D orientation classification results may indicate that all visual areas showed the similar patterns between objects with different pitch angles and same roll angles. Only POIPS showed relatively high decoding accuracy from occluded full grasping action. This suggests that the decoded 3D orientation cortical pattern is from action-related process in this area. Overall, our findings suggest that, with different grasping action types, the V1, V2, V3d, and some IPS areas are involved in the orientation representation and vary along the dorsal pathway, from vision-related to action-related, during occluded action.

2.6.1 Orientation Representation from Early to Higher Visual Areas

2.6.1.1 Visual processing in V1 and V2

In blinded actions, when performed, there is activation in the EVC (Raos & Savaki, 2010; Kilintari et al., 2011; Singhal et al., 2013). Recently, the studies using MVPA to find the action representation in the EVC (Gallivan et al., 2019, Velji‐Ibrahim et al., 2022) suggested the presence of feedback signals from motor-related areas to visual areas during action tasks, which may serve for processing specific information about the visual features of an object, important for the execution of incoming actions. Our results indicated that the orientation representation in V1 and V2 during occluded grasping suggests the presence of feedback

signals as well. In addition, the representation of orientation can be cross decoded across grasping types in V1 and V2 during occluded action. Although, some limitations have been found in approaches that cross-decode between different action conditions (Monaco et al., 2020), the orientation representations found in these areas were unaffected by the cross-decoding. This suggests that only the visual-related orientation representation (visual image of an object) was decoded in these areas. Additionally, Gutteling et al. (2011) found that orientation processing can be enhanced by action preparation in the EVC, which may be due to feedback signals from motor-related areas. Our findings on the significantly high decoding accuracy in V1 may support this idea.

2.6.1.2 Action-related processing in V3d

In the study of Kilintari et al. (2011), the activation was found in V3d and V3A during the blind reach to grasp a 3D object in rhesus monkeys, suggesting that these activations reflect visuospatial information for reaching and object-related information for grasping. This may corroborate our results, as object orientation may be considered object-related information for "occluded grasping," which removed the visibility of an object in similar case to "blind grasp." Furthermore, in their study, they identified that the occipitoparietal segment of monkey V3d area showed more activation during action execution in the dark than in light from the imagery of action tasks. In addition, the previous study suggested the representation from the somatosensory input and action process to feedback signals to V3d while performing the non-visually guided grasp (Threethipthikoon et al., 2023). This may explain the non-significant decoding accuracy of the transfer-type in the action phase observed in our V3d results. The mental imagery associated with full and precise grasps may differ enough to make the cortical pattern unable to be transferred. Conversely, the lower visual field preference for the action process in the dorsal pathway may affect the orientation representation in V3d. Since V3d is located in early dorsal area and is associated with the lower visual field, which is related to limb positioning for visuomotor control tasks and processing objects in peri-personal space (Previc, 1990; Danckert & Goodale, 2001, 2003). This may explain how the orientation process showed the significance in dorsal area V3d and non-significant in ventral area V3v. Hence, we hypothesize that V3d may include both the representation of vision-related and action-related orientation. The vision-related orientation representation was revealed from the vision phase with a similar retinotopic organization process to the V1 and V2 from transfer-type results. The action-related orientation

representation was revealed from the action phase based on the failed to transfer decoding of the specific cortical pattern of each grasping type.

2.6.1.3 Grasping types and IPS areas

In the present study, the full grasping type mainly showed the high decoding accuracy overall in each ROI (Figure 2.5B). Previous studies have shown differences in brain activation between precise grasp and whole hand grasp in primary motor cortex, premotor, and parietal areas (Ehrsson et al., 2000, 2001). Precise grips require the calculation of object data such as shape, size, and orientation before execution (Castiello, 2005). Moreover, the human anterior intraparietal sulcus, which is selective to visually guided tasks, shows higher activation when using precise grasping on small objects than when performing whole hand grasps (Begliomini et al., 2007). Additionally, recent study found that the low richness of visual feedback for the hand decreases grasp performance, particularly in precise grasping (Sivakumar et al., 2021). These studies suggest that precise grasping relies more on the online visual feedback to execute action, while full grasping may depend less on the visual input and more on other signals from feedback processing or other sensory input. For example, proprioceptive information may be more important in a full grasp, as it provides information about the hand's position and movement in space. Moreover, in non-visual guided grasping, proprioceptively guided grasping showed weak activation in the anterior intraparietal sulcus (Fabbri et al., 2014). Furthermore, our results suggest that the visual dependency for precise grasping might be more apparent in the VIPS and DIPS, as indicated by the relatively considerable difference in orientation decoding results between precise and full grasping types (Figure 2.5B) <direct compare need change. In addition, with full grasping, VIPS and DIPS displayed significantly and relatively high decoding results for 2D orientation (Figure 2.5B) and in POPIS for 3D orientation, which in the latter decoding results was not observed significance in other ROIs (Figure 2.6B). These results may suggest that the 3D orientation cortical pattern of POIPS areas may be more distinctive during grasping than visual observation. Therefore, during an occluded grasp, VIPS and DIPS, where the visual dependency for precise grasping tends to be more pronounced, may rely on the action-related process for orientation representation.

2.6.1.4 Ventral areas (V3v and LOC)

The ventral visual areas showed non-significant orientation representation. In the same-type

classification, the decoding results from V3v and LOC showed non-significance both in the vision and action phases (Figure 2.5A, 2.5B). However, the transfer-type classification decoding results of these areas showed significantly high results in the action phase (Figure 2.5C). The high accuracy decoding of transfer-type results may indicate generalizable features that are not specific to a particular grasping type, which may be the visual recognition related process found in the ventral stream pathway evoked by the occluded action. A similar activation was previously observed in LOC while executing an action in complete darkness, and was suggested that the evoked BOLD signal was caused by the detailed visual representation of object for the motor coding (Singhal et al., 2013). Although our results from V3v and LOC showed a tendency of the representation in visual recognition of object orientation from high decoding accuracy, further investigation is needed for the visual recognition aspect.

2.6.1.5 Laterality of occluded grasping

During the vision phase, we observed an influence of retinotopic organization in bilateral early visual areas (Figure 2.7A-1, 2.7A-2). While the decoding accuracy was relatively lower than that of the combined ROI results, the decoding tendency showed consistent patterns. This decrease in accuracy could be attributed to utilization of only half of the data in MVPA, potentially leading to increased noise, affecting precise of the decoding. In the action phase, our investigation yielded significant decoding results from V3d, V3A, VIPS, and DIPS—particularly in the context of the full grasping type—which align well with the original combined ROI results (Figure 2.7B-1, 2.7B-2). Furthermore, the analysis comparing the two hemispheres showed no significant differences, suggesting limited evidence of consistent laterality in our data.

2.6.2 Limitations

The visually occluded grasping includes multiple sensory inputs. Tactile and proprioceptive information, such as the sense of touch when the hand reaches toward an object, as well as information from the hand orientation, may assist for orientation. Haptic shape exploration showed activation in retinotopic visual areas, which appeared for guiding the grasp toward an object (Monaco et al., 2017). In a study using hand aligning and reaching (Velji‐Ibrahim et

al., 2022), the object features of orientation and location were modulated by action planning in the anterior and posterior parietal cortex. However, the EVC showed this modulation only with hand aligning. In our study, the full grasp may give a similar posture to the aligned hand toward the 3D object, and the orientation representation was found by full grasping even without visual guidance in visual areas. Here, we consider that feedback signals from motor-related areas are used for processing specific action tasks in absence of visual information.

In addition, the grasping posture in the experimental design may not have been entirely representative of a natural posture. The visual presentation of the object was conveyed through a two-mirror setup (Figure 2.1E), which may have resulted in a discrepancy between the grasping angle and the viewing angle. This non-natural posture may have impacted the orientation discrimination. However, the participants were provided with the opportunity to familiarize themselves with the different object orientations through visually guided practice before the start of each type of grasping session.

Another limitation of our study is the small sample size of only 10 participants, which may raise concerns regarding the generalizability of the findings. However, previous studies employing MVPA techniques have used similar sample sizes. For example, Gutteling et al. (2015) studied grasping in six participants and Harrison and Tong (2009) focused on orientation-related visual memories in a sample of <10 participants. Our previous studies (Li & Shigemasu, 2019, 2021) also utilized small sample sizes in their experimental design. Based on this knowledge, we designed our study to recruit 10 participants, given the available resources and requirements of the experimental setup. A post hoc power analysis of all MVPA results demonstrates a statistical power exceeding 0.7 for all significant findings. The lowest power value (1 - β err prob) of 0.716 was observed in DIPS, derived from the transfer-type 2D orientation classification in the action phase. In contrast, hMT+ exhibited the highest power (1 - β err prob) of 0.860 among the non-significant results, derived from the same-type 2D orientation classification of the full grasping type in the action phase. The robust statistical power observed for significant findings despite the small sample size supports the reliability and validity of our conclusions. Full details of the power analysis are provided in the supplementary materials.

2.7 References of CHAPTER 2

16. Begliomini, C., Wall, M. B., Smith, A. T., & Castiello, U. (2007). Differential cortical activity for precision and whole‐hand visually guided grasping in humans. European Journal of Neuroscience, 25(4), 1245‐1252. https://doi.org/10.1111/j.1460-9568.2007.05365.x
17. Benjamini, Y., & Yekutieli, D. (2001). The control of the false discovery rate in multiple testing under dependency. The Annals of Statistics, 29(4). https://doi.org/10.1214/aos/1013699998
18. Binkofski, F., Dohle, C., Posse, S., Stephan, K. M., Hefter, H., Seitz, R. J., & Freund, H. J. (1998). Human anterior intraparietal area subserves prehension. Neurology, 50(5), 1253–1259. https://doi.org/10.1212/wnl.50.5.1253
19. Castiello, U. (2005). The neuroscience of grasping. Nature Reviews Neuroscience, 6(9), 726–736. https://doi.org/10.1038/nrn1744
20. Cavina-Pratesi, C., Goodale, M. A., & Culham, J. C. (2007). FMRI Reveals a Dissociation between Grasping and Perceiving the Size of Real 3D Objects. PLoS ONE, 2(5), e424. https://doi.org/10.1371/journal.pone.0000424
21. Culham, J. C., Danckert, S. L., Souza, J. F. X. D., Gati, J. S., Menon, R. S., & Goodale, M. A. (2003). Visually guided grasping produces fMRI activation in dorsal but not ventral stream brain areas. Experimental Brain Research, 153(2), 180–189. https://doi.org/10.1007/s00221-003-1591-5
22. Danckert, J. A., & Goodale, M. A. (2003). Ups and downs in the visual control of action. In S. H. Johnson-Frey (Ed.), Taking action: Cognitive neuroscience perspectives on intentional acts (pp. 29–64). The MIT Press.
23. Danckert, J. A., & Goodale, M. A., (2001). Superior performance for visually guided pointing in the lower visual field. Experimental Brain Research, 137(3–4), 303–308. https://doi.org/10.1007/s002210000653
24. DeYoe, E. A., Carman, G. J., Bandettini, P., Glickman, S., Wieser, J., Cox, R., . . . Neitz, J. (1996). Mapping striate and extrastriate visual areas in human cerebral cortex. Proceedings of the National Academy of Sciences, 93(6), 2382–2386. https://doi.org/10.1073/pnas.93.6.2382
25. Dupont, P. (1997). The kinetic occipital region in human visual cortex. Cerebral Cortex, 7(3), 283–292. https://doi.org/10.1093/cercor/7.3.283

26. Ehrsson, H. H., Fagergren, A., Jonsson, T., Westling, G., Johansson, R. S., & Forssberg, H. (2000). Cortical Activity in Precision- Versus Power-Grip Tasks: An fMRI Study. Journal of Neurophysiology, 83(1), 528–536. https://doi.org/10.1152/jn.2000.83.1.528
27. Ehrsson, H. H., Fagergren, A., & Forssberg, H. (2001). Differential Fronto-Parietal Activation Depending on Force Used in a Precision Grip Task: An fMRI Study. Journal of Neurophysiology, 85(6), 2613–2623. https://doi.org/10.1152/jn.2001.85.6.2613
28. Fabbri, S., Strnad, L., Caramazza, A., & Lingnau, A. (2014). Overlapping representations for grip type and reach direction. NeuroImage, 94, 138–146. https://doi.org/10.1016/j.neuroimage.2014.03.017
29. Fabbri, S., Stubbs, K. M., Cusack, R., & Culham, J. C. (2016). Disentangling Representations of Object and Grasp Properties in the Human Brain. Journal of Neuroscience, 36(29), 7648–7662. https://doi.org/10.1523/jneurosci.0313-16.2016
30. Faillenot, I. (1997). Visual pathways for object-oriented action and object recognition: functional anatomy with PET. Cerebral Cortex, 7(1), 77–85. https://doi.org/10.1093/cercor/7.1.77
31. Fischl, B. (2012). FreeSurfer. NeuroImage, 62(2), 774–781. https://doi.org/10.1016/j.neuroimage.2012.01.021
32. Gallivan, J. P., Chapman, C. S., Gale, D. J., Flanagan, J. R., & Culham, J. C. (2019). Selective Modulation of Early Visual Cortical Activity by Movement Intention. Cerebral Cortex, 29(11), 4662–4678. https://doi.org/10.1093/cercor/bhy345
33. Goodale, M. A., & Milner, A. (1992). Separate visual pathways for perception and action. Trends in Neurosciences, 15(1), 20–25. https://doi.org/10.1016/0166-2236(92)90344-8
34. Gutteling, T. P., Kenemans, J. L., & Neggers, S. F. W. (2011). Grasping Preparation Enhances Orientation Change Detection. PLoS ONE, 6(3), e17675. https://doi.org/10.1371/journal.pone.0017675
35. Gutteling, T. P., Park, S. Y., Kenemans, J. L., & Neggers, S. F. W. (2013). TMS of the anterior intraparietal area selectively modulates orientation change detection during action preparation. Journal of Neurophysiology, 110(1), 33–41. https://doi.org/10.1152/jn.00622.2012
36. Gutteling, T. P., Petridou, N., Dumoulin, S. O., Harvey, B. M., Aarnoutse, E. J., Kenemans, J. L., & Neggers, S. F. (2015). Action Preparation Shapes Processing in Early Visual Cortex. The Journal of Neuroscience, 35(16), 6472–6480. https://doi.org/10.1523/jneurosci.1358-14.2015

37. Harrison, S. A., & Tong, F. (2009). Decoding reveals the contents of visual working memory in early visual areas. Nature, 458(7238), 632–635. https://doi.org/10.1038/nature07832
38. Kilintari, M., Raos, V., & Savaki, H. E. (2011). Grasping in the Dark Activates Early Visual Cortices. Cerebral Cortex, 21(4), 949–963. https://doi.org/10.1093/cercor/bhq175
39. Kourtzi, Z., & Kanwisher, N. (2000). Cortical Regions Involved in Perceiving Object Shape. The Journal of Neuroscience, 20(9), 3310–3318. https://doi.org/10.1523/jneurosci.20-09-03310.2000
40. Kourtzi, Z., & Kanwisher, N. (2001). Representation of Perceived Object Shape by the Human Lateral Occipital Complex. Science, 293(5534), 1506–1509. https://doi.org/10.1126/science.1061133
41. Li, Z., & Shigemasu, H. (2019). Generalized Representation of Stereoscopic Surface Shape and Orientation in the Human Visual Cortex. Frontiers in Human Neuroscience, 13. https://doi.org/10.3389/fnhum.2019.00283
42. Li, Z., & Shigemasu, H. (2021). Unique Neural Activity Patterns Among Lower Order Cortices and Shared Patterns Among Higher Order Cortices During Processing of Similar Shapes With Different Stimulus Types. i-Perception, 12(3), 204166952110182. https://doi.org/10.1177/20416695211018222
43. Marangon, M., Kubiak, A., & Króliczak, G. (2016). Haptically Guided Grasping. fMRI Shows Right-Hemisphere Parietal Stimulus Encoding, and Bilateral Dorso-Ventral Parietal Gradients of Object- and Action-Related Processing during Grasp Execution. Frontiers in Human Neuroscience, 9. https://doi.org/10.3389/fnhum.2015.00691
44. Mishkin, M., Ungerleider, L. G., & Macko, K. A. (1983). Object vision and spatial vision: two cortical pathways. Trends in Neurosciences, 6, 414–417. https://doi.org/10.1016/0166-2236(83)90190-x
45. Monaco, S., Cavina-Pratesi, C., Sedda, A., Fattori, P., Galletti, C., & Culham, J. C. (2011). Functional magnetic resonance adaptation reveals the involvement of the dorsomedial stream in hand orientation for grasping. Journal of Neurophysiology, 106(5), 2248–2263. https://doi.org/10.1152/jn.01069.2010
46. Monaco, S., Gallivan, J. P., Figley, T. D., Singhal, A., & Culham, J. C. (2017). Recruitment of Foveal Retinotopic Cortex During Haptic Exploration of Shapes and Actions in the Dark. The Journal of Neuroscience, 37(48), 11572–11591. https://doi.org/10.1523/jneurosci.2428-16.2017

47. Monaco, S., Malfatti, G., Culham, J. C., Cattaneo, L., & Turella, L. (2020). Decoding motor imagery and action planning in the early visual cortex: Overlapping but distinct neural mechanisms. NeuroImage, 218, 116981 https://doi.org/10.1016/j.neuroimage.2020.116981
48. Murata, A., Gallese, V., Luppino, G., Kaseda, M., & Sakata, H. (2000). Selectivity for the Shape, Size, and Orientation of Objects for Grasping in Neurons of Monkey Parietal Area AIP. Journal of Neurophysiology, 83(5), 2580–2601. https://doi.org/10.1152/jn.2000.83.5.2580
49. Orban, G. A. (2016). Functional definitions of parietal areas in human and non-human primates. Proceedings of the Royal Society B: Biological Sciences, 283(1828), 20160118. https://doi.org/10.1098/rspb.2016.0118
50. Petro, L. S., Vizioli, L., & Muckli, L. (2014). Contributions of cortical feedback to sensory processing in primary visual cortex. Frontiers in Psychology, 5. https://doi.org/10.3389/fpsyg.2014.01223
51. Previc, F. H. (1990). Functional specialization in the lower and upper visual fields in humans: Its ecological origins and neurophysiological implications. Behavioral and Brain Sciences, 13(3), 519–542. https://doi.org/10.1017/s0140525x00080018
52. Rice, N. J., Valyear, K. F., Goodale, M. A., Milner, A. D., & Culham, J. C. (2007). Orientation sensitivity to graspable objects: An fMRI adaptation study. NeuroImage, 36, T87–T93. https://doi.org/10.1016/j.neuroimage.2007.03.032
53. Sereno, M. I., Dale, A. M., Reppas, J. B., Kwong, K. K., Belliveau, J. W., Brady, T. J., Rosen, B. R., & Tootell, R. B. (1995). Borders of multiple visual areas in humans revealed by functional magnetic resonance imaging. Science (New York, N.Y.), 268(5212), 889–893. https://doi.org/10.1126/science.7754376
54. Singhal, A., Monaco, S., Kaufman, L. D., & Culham, J. C. (2013). Human fMRI Reveals That Delayed Action Re-Recruits Visual Perception. PLoS ONE, 8(9), e73629. https://doi.org/10.1371/journal.pone.0073629
55. Sivakumar, P., Quinlan, D. J., Stubbs, K. M., & Culham, J. C. (2021). Grasping performance depends upon the richness of hand feedback. Experimental Brain Research, 239(3), 835–846. https://doi.org/10.1007/s00221-020-06025-0
56. Threethipthikoon, T., Li, Z., & Shigemasu, H. (2023). Orientation representation in human visual cortices: contributions of non-visual information and action-related process. Frontiers in Psychology, 14. https://doi.org/10.3389/fpsyg.2023.1231109
57. Valyear, K. F., Culham, J. C., Sharif, N., Westwood, D., & Goodale, M. A. (2006). A

double dissociation between sensitivity to changes in object identity and object orientation in the ventral and dorsal visual streams: A human fMRI study. Neuropsychologia, 44(2), 218–228. https://doi.org/10.1016/j.neuropsychologia.2005.05.004

58. Vanduffel, W., Fize, D., Peuskens, H., Denys, K., Sunaert, S., Todd, J. T., & Orban, G. A. (2002). Extracting 3D from Motion: Differences in Human and Monkey Intraparietal Cortex. Science, 298(5592), 413–415. https://doi.org/10.1126/science.1073574
59. Velji‐Ibrahim, J., Crawford, J. D., Cattaneo, L., & Monaco, S. (2022). Action planning modulates the representation of object features in human fronto‐parietal and occipital cortex. European Journal of Neuroscience, 56(6), 4803‐4818. https://doi.org/10.1111/ejn.15776
60. Warnking, J., Dojat, M., Guérin-Dugué, A., Delon-Martin, C., Olympieff, S., Richard, N., Chéhikian, A., & Segebarth, C. (2002). fMRI retinotopic mapping--step by step. NeuroImage, 17(4), 1665–1683. https://doi.org/10.1006/nimg.2002.1304
61. Zeki, S., Perry, R. J., & Bartels, A. (2003). The processing of kinetic contours in the brain. Cerebral cortex (New York, N.Y. : 1991), 13(2), 189–202. https://doi.org/10.1093/cercor/13.2.189
62. Zeki, S., Watson, J. D., Lueck, C. J., Friston, K. J., Kennard, C., & Frackowiak, R. S. (1991). A direct demonstration of functional specialization in human visual cortex. The Journal of neuroscience : the official journal of the Society for Neuroscience, 11(3), 641–649. https://doi.org/10.1523/JNEUROSCI.11-03-00641.1991

CHAPTER 3

Topic 2: Orientation Representation in Human Visual Cortices: Contributions of Non-Visual Information and Action-Related Process

3.1 Abstract

Orientation processing in the human brain plays a crucial role in guiding grasping actions toward an object. Remarkably, despite the absence of visual input, the human visual cortex can still process orientation information. Instead of visual input, non-visual information, including tactile and proprioceptive sensory input from the hand and arm, as well as feedback from action-related processes, may contribute to orientation processing. However, the precise mechanisms by which the visual cortices process orientation information in the context of non-visual sensory input and action-related processes remain to be elucidated. Thus, our study examined the orientation representation within the visual cortices by analyzing the blood-oxygenation-level-dependent (BOLD) signals under four action conditions: direct grasp (DG), air grasp (AG), non-grasp (NG), and uninformed grasp (UG). The images of the cylindrical object were shown at +45° or -45° orientations, corresponding to those of the real object to be grasped with the whole-hand gesture. Participants judged their orientation under all conditions. Grasping was performed without online visual feedback of the hand and object. The purpose of this design was to investigate the visual areas under conditions involving tactile feedback, proprioception, and action-related processes. To address this, a multivariate pattern analysis was used to examine the differences among the cortical patterns of the four action conditions in orientation representation by classification. Overall, significant decoding accuracy over chance level was discovered for the DG; however, during AG, only the early visual areas showed significant accuracy, suggesting that the object's tactile feedback influences the orientation process in higher visual areas. The NG showed no statistical significance in any area, indicating that without the grasping action, visual input does not

contribute to cortical pattern representation. Interestingly, only the dorsal and ventral divisions of the third visual area (V3d and V3v) showed significant decoding accuracy during the UG despite the absence of visual instructions, suggesting that the orientation representation was derived from action-related processes in V3d and visual recognition of object visualization in V3v. The processing of orientation information during non-visually guided grasping of objects relies on other non-visual sources and is specifically divided by the purpose of action or recognition.

3.2 Introduction

Upon grasping an object, the human brain has a remarkable capacity to process information related to its orientation, even when such information is partially or completely obscured from view (Sathian and Zangaladze, 2002; Kilintari et al., 2011). The grasping action onto an object enhances the visual processing of action-relevant features like orientation from the visually guided grasping task (Bekkering and Neggers, 2002; Smith and Soechting, 2005; van Elk et al., 2010; Gutteling et al., 2011). In neuroimaging studies, signal activation during the grasp action has been found in the early visual cortex and the dorsal and ventral pathways (Binkofski et al., 1998; Murata et al., 2000; Culham et al., 2003; van Elk et al., 2010; Gutteling et al., 2015). The activation of the visual areas was further observed during grasping in a dark environment, suggesting that the visuospatial information of an object remains useful for grasping even without online visual input (Singhal et al., 2013; Marangon et al., 2016; Monaco et al., 2017). Specifically, in monkeys, activation was detected in the V3d area when grasping objects in the dark, as previously observed (Kilintari et al., 2011). It has been suggested that the cause of action-related activation in the visual areas is the feedback signals from motor-related areas (Petro et al., 2014). In addition to feedback signals from the motor system, other sources of feedback signals may come from the sensory input when action is taken.

The sensory input from action may be associated with tactile or proprioceptive sensations. Previous studies have shown that orientation discrimination based on tactile sensations involves the visual cortex (Zangaladze et al., 1999; Sathian and Zangaladze, 2002; van der Groen et al., 2013). However, when considering the orientation process from the grasping action, the tactile sensation from touching may be combined with the proprioceptive sensation of the hand position in the peripersonal space. Studies have also demonstrated that hand

orientation during reach-to-grasp movements activates the posterior intraparietal sulcus in humans, indicating the involvement of wrist components in object manipulation (Faillenot et al., 1997; Monaco et al., 2011). Furthermore, when pantomime grasping was performed while the eyes were fixated on an object, activation was observed in the anterior intraparietal sulcus area (Króliczak et al., 2007). According to previous studies, tactile and proprioceptive sensations contribute to the orientation process when grasping an object.

On the other hand, apart from sensory input, the feedback signals of action-related processes from the motor system may activate visual information in visual areas. Action-related processes, such as action planning during visuomotor tasks, are found in early visual areas and areas of the intraparietal sulcus (IPS) (Gutteling et al., 2015; Gallivan et al., 2019; Monaco et al., 2020). In addition, action planning in the anterior and posterior parietal cortices modulates the orientation and location of the object during hand alignment and reaching toward an object with a rod-like shape. However, this modulation is only observed in the early visual areas during hand alignment (Velji‐Ibrahim et al., 2022). This suggests that action-related processes in visual areas play a role in object-related orientation information.

Despite the extensive research conducted on human visual areas for processing object orientation, the exact mechanisms remain to be elucidated. Without online visual guidance, grasping involves a complex interplay of multiple processes using visual information to process the orientation of an object. To address these gaps, we investigated orientation representation regarding the sensory input and action-related process to understand the factors influencing orientation when online visual guidance is not available. We focused on tactile and proprioceptive sensations as potential non-visual sensory inputs, as well as the processes involved in orientation-related planned and unplanned grasping, to determine their effect on the representation of orientation in visual areas.

Our study aimed to investigate the orientation representation of grasping without online visual guidance in the visual areas. We aimed to determine how representation is affected by input from the non-visual sensory system and signals from action-related processes. The multi-voxel pattern analysis (MVPA) method was used to analyze the blood-oxygenation-level-dependent (BOLD) signals obtained from the fMRI experiments. MVPA was used to decode the pattern differences for conditions in which higher-order visual areas had lower activation signals in the univariate method. The object used in the experiment had an elongated cylindrical shape, which is relevant to the grasping action in the dorsal and ventral visual streams (Fabbri et al., 2016). The object to be grasped was presented in two orientations, which were shown in a random order. Later, in the action phase, participants

performed one of the four action conditions designed to integrate the non-visual sensation and action-related processes. The action conditions were as follows: grasping an object after instruction with or without object presence, withholding grasping after instruction, and grasping an object without instruction. The first two conditions integrated proprioceptive information while having a difference in tactile feedback from the presence of the object during grasping. The third condition integrates the action-related processes while withholding the grasp. Finally, the fourth condition involved passive orientation information from proprioceptive and tactile information from the grasping action only, without orientation instruction (Table 3.1 and Figure 3.1D). We used the MVPA decoding method to determine the differences in patterns for each action condition. The decoding method was defined as the classification of orientation pairs in each region of interest (ROI) to represent the orientation process of that area. In addition, transfer-type classification or cross-decoding was performed to identify shared patterns across action conditions related to the orientation process. If the results of the transfer classification are statistically significant, it indicates that the area contains a generalization of the sensory-related representation or action-related processes representation. Based on previous research, the early visual and IPS areas were assumed to have high decoding accuracy in the instructed grasp conditions, considering that the planned action can enhance the orientation process (Gutteling et al., 2015). The early visual areas were assumed to be less affected by tactile feedback because visual information is mainly processed in these areas more than somatosensory information. In the dorsal division of the third visual area (V3d), we anticipated a high decoding accuracy during grasping without instruction. We based this assumption on previous findings that demonstrated activation in V3d during the processing of visuospatial information in the dark, in the absence of visual stimuli, suggesting an action-related process (Kilintari et al., 2011). Finally, both the V3d and IPS areas were considered candidates for cross-decoding between grasping with and without instruction from the action-relevant features within the dorsal visual pathway areas (Culham et al., 2003; Singhal et al., 2013).

3.3 Methodology

3.3.1 Participants

A group of ten participants (five females, five males; age mean ± SD, 25.94 ± 3.727) were recruited from Kochi University of Technology, Japan, to participate in the fMRI experiments. The selection criteria included having a normal or corrected-to-normal vision and being free from mental illness or neurological disease. Prior to participating, all participants provided written informed consent, in accordance with the Declaration of Helsinki. All participants were compensated for their participation. The study protocol was reviewed and approved by the Human Research Ethics Committee of the Kochi University of Technology.

3.3.2 Experimental Design

The fMRI experiment was designed to investigate the effect of the sensory input and motor output on the processing of orientation during grasping with no online visual feedback. The four action conditions were intended to be used for this investigation and were defined as a combination of visual instructions and the task assigned during the action phase. These action conditions were grasping objects after observation (direct grasp condition [DG]), grasping with no object present after observation (air grasp condition [AG]), withholding grasping after observation (non-grasp condition [NG]), and grasping objects without instructions (uninformed grasp [UG]). The DG condition integrated all tactile input and visual instruction, the AG condition had no tactile feedback of the grasping object, the NG condition had action planning but stopped the execution, and lastly, the UG condition had no planning from visual instruction and the participants perceived the orientation of the object from action only (Table 3.1).

In experimental design, each trial comprised of three phases instruction, action, and judgment (Figure 3.1C). During the instruction phase, participants were presented with the stimulus of an object in two different orientations, either left or right, for a duration of 1 s. Alternatively, for the UG condition, a black fixation cross was presented instead of the object stimulus, for the same duration. Subsequently, the instruction phase was followed by a blue fixation cross signaling a waiting period of 5 s before the commencement of the next phase. The next phase was the action phase, where participants were presented with a green or red fixation cross for

a duration of 4 s. The green or red cross respectively signaled the participants to either perform a whole-hand grasp or withhold a grasp. All action conditions were performed on the green cross except for the NG condition. The DG condition had a real object for grasping, whereas, in the AG condition, participants made the grasping gesture in the absence of an object. In the NG condition, the participants withheld their grasp during this phase. In the UG condition, participants grasped an object without knowing its orientation. Subsequently, the participants saw the blue fixation cross for a duration of 8 s, waiting for the next phase. During the judgment phase, participants were presented with the stimuli of the object in both orientations, which were randomly ordered. They were prompted to select the correct orientation that they had either previously grasped or observed for a duration of 2 s. Keypads were used for the binary choice of left and right buttons (Figure 3.1E). Finally, the blue fixation cross was presented again for a duration of 4 s until the commencement of the next trial. A detailed illustration of the trial is shown in Figures 3.1C and 3.3A.

All experiments were conducted in a single session. Each session comprised 10 runs, each run consisted of 16 trials, and each trial was further divided into three distinct phases: instruction, action, and judgment (Figure 3.1C). During the instruction phase, participants were presented with the stimuli of an object. In the subsequent action phase, participants performed an action according to the orientation in the previous phase. Finally, in the judgment phase, participants pressed a button selecting the corresponding orientation (Figure 3.1C). Each trial had eight possible settings (2 orientations x 4 action conditions) using an event-related design paradigm. The trials were repeated 20 times. All the participants performed 160 trials (2 orientations x 4 action conditions x 20 repetitions). The action conditions used the same timing diagram but with different visual stimuli and actions (Figure 3.1D).

To calculate the orientation perception performance of each participant, the responses to all judgment tasks per run were recorded. Unanswered assignments were excluded from calculations. All participants were instructed to fixate on the fixation cross at the center of the screen. Any runs with excessive head movements were eliminated. Extraordinary head movement was defined as a head movement greater than 2 mm and/or head rotation greater than 2° from the initial scan of each run. All participants remained still for at least eight echo-planar imaging (EPI) runs. During the session, three participants who were experiencing fatigue took a break in the middle of the session to alleviate their fatigue before continuing with the remaining session.

Table 3.1 The estimate functions of sensory input and action-related processes to each action condition

	Tactile feedback	Proprioception	Action plan	Visual working memory
Direct Grasp (DG)	✓	✓	✓	✓
Air Grasp (AG)		✓	✓	✓
Non-grasp (NG)				✓
Uninformed Grasp (UG)	✓	✓		

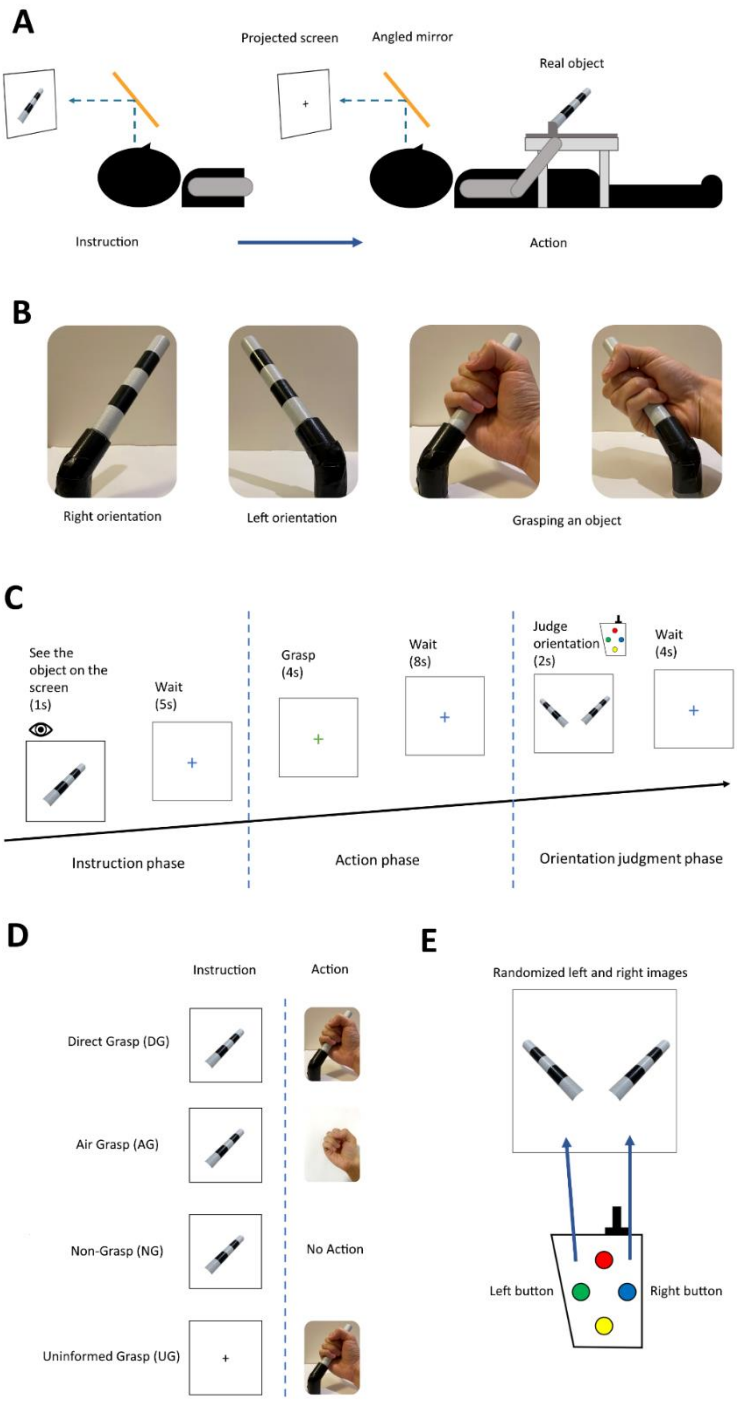

Figure 3.1. A) Experimental setup: the participant sees the projected stimulus through the angled mirror setup located above the head coil. The photograph of the object was shown for a direct angle presentation of the object in each orientation. B) The object used in the experiment and two orientations with grasping gesture. The object rotated in roll axis of +45° and −45° by the experimenter. C) Experimental diagram displaying the trial in the experimental session. D) The four action conditions for grasping an object with difference in instruction and action phases. E) The stimuli for button pressing choice in the orientation judgment phase. Participant selected the presents orientation that corresponded to previously grasped or observed object.

3.3.3 Stimuli

Participants observed the stimuli through an angled mirror situated above the head coil. The mirror displayed a screen that presented the stimuli from a projector (Figure 3.1A). The participants' visual input was from this setting for the entire experiment, without seeing the real object situated in their hip area. An MR-compatible keypad was used to collect judgment choices in the judgment phase. All participants practiced all the action conditions prior to the start of the experiment.

The object for grasping was placed on the table around the participant's hip area, and the object was fixed on a wooden frame to maintain the position of the correct orientation (Figure 3.1A). The wooden frame was placed on a plastic table. The keypad was fixed to the right side of a wooden frame on the table. The participants used their right hand to grasp and press the required button.

The experimental stimulus used in this study was a cylindrical object made of plastic and adorned with black and white stripes. The dimensions of the object were 12.5 cm by 1.8 cm in length and diameter. The object was positioned in two different orientations, rotated in a combination of +45° or −45° on the roll axis (Figure 3.1B). The photograph of the object was projected on the screen as the visual instruction and eventual choice in the judgment phase. During the instruction phase, the image of the object was presented at the center of the screen. In the judgment phase, two images of the object, each depicting one of the two possible orientations, were presented on the left and right sides of the screen, with a black square at the bottom of both images. The black square changed to a green square when the corresponding button was pressed, indicating the participant's selection. The order of the images was randomized for each trial.

3.3.4 fMRI Data Acquisition

All imaging scans were performed using a 3 Tesla Siemens MAGNETOM Prisma MRI scanner at the Brain Communication Research Center of Kochi University of Technology. Participants' head movements were minimized by securing their heads with MRI-compatible foam pads. Each participant underwent a high-resolution T1-weighted anatomical scan (1 mm3), and ROIs were localized and delineated in all separate sessions. During each experimental run, BOLD signals were measured using an EPI sequence with the following parameters: echo time (TE), 58 ms; repetition time (TR), 2,000 ms; 198 volumes per run; 3

mm slice thickness; and interleaved slice acquisition order. The visual, posterior parietal, and posterior temporal cortices were each covered with 34 slices. Additionally, a T2-weighted structural image was acquired for each participant in a 2.5-minute run before the corresponding EPI data in one session. The T2-weighted structural data served as reference slices for the motion correction of the EPI data and co-registration between the T1-weighted anatomical images and EPI data in the native anatomical space. Finally, all data were converted to Talairach coordinates.

The primary objective of our study was to examine the representation of orientation within visual areas under four action conditions in which the object was not visible during grasping (Figure 3.2A). Following the localizer protocol, retinotopically localized early visual areas (V1, V2, V3d, V3v, and V3A) were individually delineated for each participant using a rotating wedge and expanding ring technique (Sereno et al., 1995; DeYoe et al., 1996; Warnking et al., 2002). Furthermore, V7 was identified as the anterior and dorsal region relative to V3A. In addition to these visual areas, we included regions within the IPS, namely the ventral intraparietal sulcus (VIPS), parieto-occipital intraparietal sulcus (POIPS), and dorsal intraparietal sulcus (DIPS). The IPS areas were identified by comparing the activity of the 3D shapes generated by a rotating motion with that of the 2D shapes generated along a frontoparallel plane (Vanduffel et al., 2002). Additionally, the anterior intraparietal area in nonhuman primates has demonstrated selectivity for the shape, size, and orientation of 3D objects during grasping (Murata et al., 2000). This area in primates has been proposed as a homolog of the human dorsal IPS based on multiple functional tests (Orban, 2016). The signal patterns obtained from each ROI were used to create the classification sample data, with patterns from both the left and right hemispheres merged to represent each ROI. Gutteling et al. (2015) reported no significant differences in contralateral visual areas from the MVPA of visually guided actions toward objects on the left and right sides. In line with this finding, our study opted to include both hemispheres in all analyses.

3.4 Data Analysis

3.4.1 Pre-Processing

Data processing and analyses were conducted using several software packages, including FreeSurfer (Fischl, 2012), BrainVoyager 21 (version 21.0.0.3720, 64-bit; BrainInnovation,

Maastricht, Netherlands), and MATLAB R2020b (The MathWorks, Natick, MA, USA). The FreeSurfer software was used to extract white matter (WM) and gray matter (GM) from T1-weighted 3D anatomical images. WM was then employed as a segmentation mask together with GM in BrainVoyager, and the resulting brain was transformed into the Talairach space to generate the cortical surface. Subsequently, the inflated cortical surface was used to define ROIs for MVPA. For the EPI data, 3D motion correction was performed using the T2-weighted image acquired at the beginning of the session without applying spatial smoothing. Co-registration between the EPI data and the T1-weighted image was performed, followed by transformation into the Talairach space.

3.4.2 ROI-Based Univariate Analysis

We performed a univariate analysis of the overall BOLD signal pattern in each ROI to observe the signal changes in each phase, which is expected to decrease in the higher-order visual areas, and we expected that the MVPA can give further distinguishable results. The average BOLD signal pattern was defined as the percentage signal change for stimuli versus baseline, grasping versus baseline, and judgment versus baseline. Additionally, the BOLD signals when no orientation instruction was given (UG condition) and no action was taken (NG condition) were separately analyzed from the average BOLD signal pattern. Three volumes were computed for the hemodynamic latency of the BOLD signal (6 seconds). For the subsequent analysis, we utilized the mean percentage of signal change across all runs and participants.

3.4.3 ROI-Based MVPA

MVPA is a widely recognized analytical approach known for its high sensitivity in detecting differences between conditions. MVPA was applied to the EPI data obtained from each ROI. To conduct MVPA classification, a linear support vector machine (SVM) was employed as a binary classifier in MATLAB. Two classification approaches were employed: same-type and transfer-type. In the same-type classification, both the training and testing of the SVM utilized the same dataset of action conditions to investigate specific cortical patterns related to the orientation of each action condition. Conversely, transfer-type classification involved training and testing the SVM with different datasets across the action conditions, such as training with the DG condition and then testing with the UG condition, and vice versa. The results obtained

from the transfer classification were used to assess the common patterns shared across the different action conditions. For each classification, pairs of distinct orientations were used as inputs for the SVM to determine the accuracy of the orientation classification. The classification accuracy was defined as the orientation classification of the respective ROI.

For each ROI, the selection of the ROI from both hemispheres involved choosing the top 250 voxels with contrast for the stimulus versus the fixation baseline. In cases where the ROI contained fewer than 250 voxels, all available voxels were included. In the instruction and judgment phases, a single volume scan was calculated after a 4-second interval. In the action phase, the average values of two volumes were calculated, taken 8 seconds after the onset, to account for the longer movement time of 4 seconds (Figure 3.3A). These differences were transformed into z-scores and used to train and test the SVM.

The leave-one-run-out method was employed to evaluate the performance of MVPA classification. Data from one run was used for testing, while data from the other runs served as the training data. This procedure was repeated for all runs and the accuracy of each iteration was averaged to determine the accuracy of the participant. Subsequently, the classification accuracies across participants were averaged for each ROI.

To determine the statistical significance of the MVPA results, a two-tailed one-sample t-test was performed across participants, with a chance level of decoding set at 50% for each ROI with a p-value threshold of 0.05. To correct for multiple comparisons (number of ROIs x number of tests) across the nine ROIs, the false discovery rate method (FDR) was applied, with an adjusted p-value threshold of 0.05 (Benjamini and Yekutieli, 2001).

3.5 Results

3.5.1 ROI-Based Univariate Analysis

A univariate analysis was conducted to ensure that the BOLD signals change occurred throughout the phases. The primary "percent signal changes" results from stimuli versus baseline, grasping versus baseline, and judgment versus baseline were high in the early visual areas, while the signals decreased toward the higher dorsal areas (Figure 3.2B). Although cortical activity was detected, the signal changes were weak along the higher-order visual areas (Figure 3.2B). The percent signal changes were significantly high (above 0) ($p < 0.0005$). A statistically significant difference among the three contrasts was not found. The percentage signal changes of UG instruction versus baseline and NG action versus baseline were lower than the average signals of all conditions (Figure 3.2C). DIPS showed no significance in NG action versus baseline. This may be due to the absence of retinal information of the object input in the visual areas and the absence of action performed as in the other three conditions. The results suggest further investigation using MVPA classification methods to assess the characteristics of each condition in each phase.

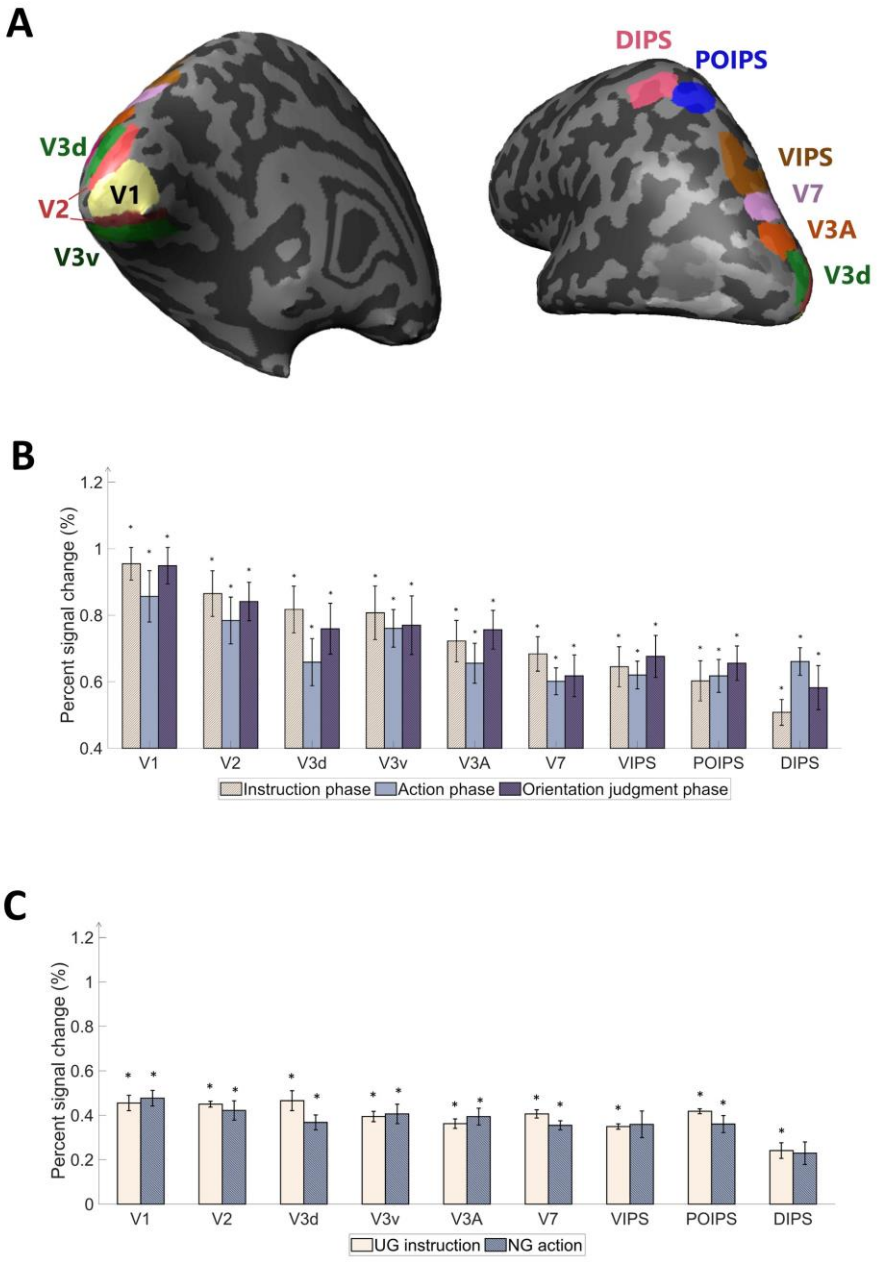

Figure 3.2 Regions of interest (ROI) used in the experiment and percentage of signal changes in the studied areas. (A) The ROIs contain areas in visual cortices. Our study's early visual cortex (EVC) includes the areas V1, V2, V3d, and V3v. The dorsal areas include V3A and V7. The intraparietal sulcus (IPS) areas comprise the ventral intraparietal sulcus (VIPS), parieto-occipital intraparietal sulcus (POIPS), and dorsal intraparietal sulcus (DIPS). The dark gray pattern indicates the sulci, whereas the light gray pattern indicates the gyri. The ROIs were individually delineated by standard localization sessions (see the fMRI acquisition section). (B) Percent signal changes of the areas using averaged BOLD data from instruction, action, and orientation judgment phases. The signal changes decrease toward the higher-order areas. (C) Percent signal changes of the areas using averaged BOLD data from UG condition in the instruction phase and NG condition in the action phase. Compared to (B) results, the signal changes had the same decreasing tendency toward higher-order areas but lower overall signal strength. The error bars represent the standard error of the mean from all participants (n = 10). The asterisk represents the percent signal changes significantly above the 0 from the t-test in group data (*$p < 0.0005$).

3.5.2 ROI-Based MVPA Results

3.5.2.1 Same-type classification

The same-type classification or decoding refers to the ability to classify the orientational difference of observed or grasped object in each visual area. If the accuracy is significant then the orientation is represented in that area. The classification process involved analyzing the BOLD signal from each ROI within the visual cortices, which was divided into three phases: instruction, action, and orientation judgment (Figure 3.3A). In the instruction phase (Figure 3.3B), the DG, AG, and NG conditions exhibited high decoding accuracy in V1 and V2; whereas, the UG condition displayed decoding accuracy close to chance levels across all areas. This observation may be attributed to the lack of visual instruction in the UG condition.

The action phase classification showed the ability to classify the orientation difference during grasping action or withhold grasping. In the action phase (Figure 3.3C), the DG condition demonstrated significantly higher accuracy in most areas, except V3v and V3A. The AG condition exhibited significantly high accuracy for V1, V2, V3v, and V3A, along with a relatively high accuracy for V3d. The NG condition displays no significant decoding accuracy for any area. In contrast, the UG condition showed significantly higher accuracy for V3d and V3v and relatively higher accuracy for V7. There are four points to be stated from these results. First, both the visual instruction and execution of the action itself showed the main contribution to decoding accuracy in V1 and V2. Second, the V3 area showed different decoding results depending on the tactile feedback of the object. Thirdly, in the V7 and IPS areas, the tactile feedback from the action affected the decoding results the most. Fourth, the withhold action (NG condition) showed that the decoded cortical pattern was affected in all areas. This suggested that the decoding results in this phase represented action-related orientation.

In the judgment phase (Figure 3.3D), V1, V2, and V3d demonstrated high accuracy, whereas the IPS areas showed non-significant accuracy in most conditions. Specifically, areas V1, V2, V3d, and V3A exhibited significant accuracy under the AG conditions. Finally, V3v displayed significantly high accuracy in the UG condition. This may indicate that decoding results were the orientation-related cortical pattern from visual image cues during judgment, action of button pressing, and evoke working memory from orientation in previous phases.

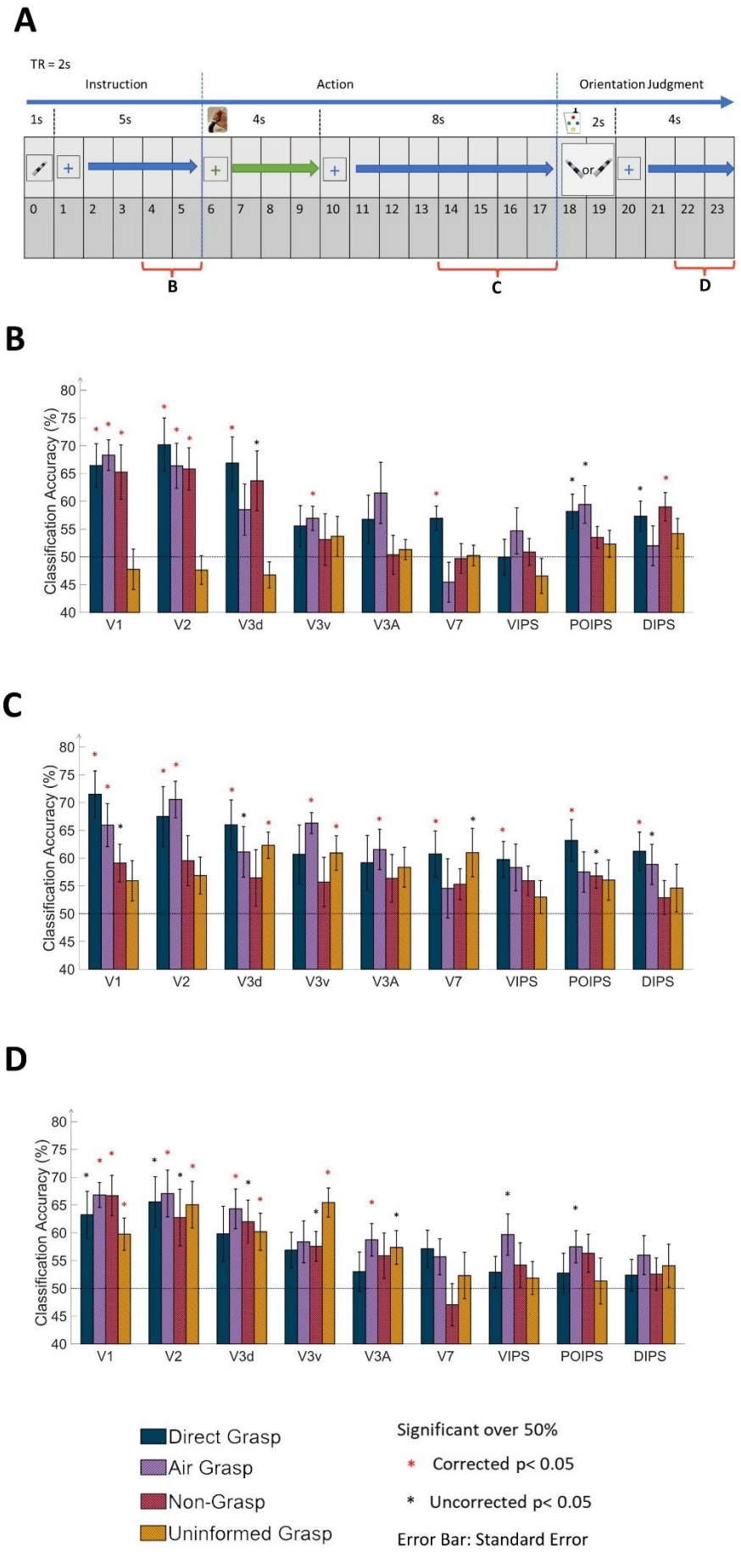
A
TR = 2s
Instruction
Action
Orientation Judgment
1s
5s
4s
8s
2s
4s
or
0 1 2 3 4 5 6 7 8 9 10 11 12 13 14 15 16 17 18 19 20 21 22 23
B
C
D
B
Classification Accuracy (%)
80 75 70 65 60 55 50 45 40
V1 V2 V3d V3v V3A V7 VIPS POIPS DIPS
C
Classification Accuracy (%)
80 75 70 65 60 55 50 45 40
V1 V2 V3d V3v V3A V7 VIPS POIPS DIPS
D
Classification Accuracy (%)
80 75 70 65 60 55 50 45 40
V1 V2 V3d V3v V3A V7 VIPS POIPS DIPS
Direct Grasp
Air Grasp
Non-Grasp
Uninformed Grasp
Significant over 50%
* Corrected p< 0.05
* Uncorrected p< 0.05
Error Bar: Standard Error

Figure 3.3 Time windows of the MVPA data and results of same-type classification with ROI-based MVPA. (A) The timing diagram of the dataset applied to MVPA classification at 6 s from the onset time in the instruction, action, and orientation judgment phases. The main dataset in the action phase covered 4 s window corresponding to the 4 s of grasping time. (B) The bar graph displays results from the MVPA classification in the instruction phase. The results showed high classification accuracy in V1, V2, V3d, and around chance level accuracy from the UG condition. (C) The bar graph displays the results in the action phase. The V1 and V2 showed high classification accuracy in DG and AG conditions. Notably, V3d and V3v showed high classification accuracy in the UG condition. (D) The bar graph displays results in the orientation judgment phase. The early visual area showed relatively high classification accuracy. In every graph, the results show all conditions of each area by classification (decoding) accuracy and areas. The dashed line indicates the chance level of the classification at 50%. The error bars represent the standard error of the mean across the participants (n = 10). The black asterisk represents the statistical significance over the chance level (50%) with two-tailed t-tests across the subjects ($p < 0.05$). The red asterisk indicates the statistical significance based on an FDR correction of $q < 0.05$.

3.5.2.2 Transfer-type classification

The results of the transfer-type classification are presented in the same order as those of the same-type classification. In the instruction phase, we conducted transfer-type classifications using the UG and other conditions as follows: “DG & UG”, “AG & UG”, and “NG & UG”. These transfer-type classifications aimed to identify common patterns associated with action preparation that may not be orientation-specific because of the absence of instructions in the UG condition. The decoded results from the selected pairs of transfer-type classifications in the instruction phase were close to the chance level. We did not perform transfer-type classification among conditions with the same stimuli instructions (DG, AG, and NG) to avoid decoding common visual cues orientation patterns.

Six transfer-type classifications were used in the action phase (Figure 3.4A). In Table 3.1, we identified the estimated functions regarding feedback of sensory input and motor system; whereas, when transfer classification was performed across conditions, we could determine what functions can be decoded. When all functions were included in the DG condition, the other conditions were similar and lacked some functions. The transfer-type classification across the DG and AG conditions revealed a common pattern related to proprioception, action planning, and possibly visual working memory regardless of tactile feedback from the object (Table 3.1). The transfer-type classification of both DG to NG and AG to NG might reflect the visual memory of the object related to the imagination of the object orientation. The common pattern observed in the DG and UG conditions indicates the common involvement of

tactile feedback and proprioception. Finally, the transfer classification between the AG and UG conditions may be related to proprioception.

Regarding the transfer-type classification results in the action phase (Figure 3.4B), the “DG & AG” transfer classification showed relatively high accuracy for V2, V3d, V3v, V3A, and POIPS. The decoded pattern from these areas may have the potential for proprioception, action planning, and visual working memory but some underlying tactile feedback patterns may not be common in the processing of orientation. The “DG & UG” transfer classification demonstrated significantly high accuracy for V2, V3v, VIPS, and DIPS. These areas had a common cortical pattern regarding tactile sensation and proprioception. Only V2 showed significantly high accuracy in the “AG & NG” transfer classification (Figure 3.4C). This area may involve visual working memory. Conversely, no significant results were found in the transfer-type classification of the “DG & NG”, “AG & UG”, or “NG & UG” conditions. These transfer classifications might not have enough common cortical patterns across conditions.

In the judgment phase, the transfer-type classification results indicated a common orientation-related pattern when selecting stimuli using buttons across action conditions. Overall, the early visual areas displayed high accuracy. The “DG & AG” transfer-type classification showed significance for V1, V2, V3d, V3A, and VIPS. Relatively high accuracy was observed in V1, V2, and V3A for the DG-to-AG conditions. The “DG & UG” conditions exhibited high accuracy for V2, V3d, and V3A. “AG & NG” transfer classification displayed high accuracy for V1, V2, V3d, and V3v. The “AG & UG” transfer classification showed significantly higher accuracy for V1, V2, and V3v. Finally, the “NG & UG” conditions yielded significant results for V1, V2, and V3d, and relatively high accuracy for V3A. Overall, the transfer classification of the judgment phase suggested the cortical pattern regarding the judgment on orientation in early visual areas and VIPS.

In addition, we additionally perform across-phase transfer classification where we perform training the data in the vision phase then test in the action phase and vice versa. This procedure was performed to check whether the orientation representation was shared across the vision and action phases. The decoding results showed significantly low accuracy below the chance level for the DG in V1, V2, and V3d. The AG condition showed significantly low accuracy below the chance level in V1, V2, V3d, and V3v, and NG conditions had significantly low accuracy below the chance level in V1, V2, and V3d areas. The cross-phase decoding results showed that the decoded representation is not same across vision and action phase but not entirely unrelated. This suggested some counter or inverse relationship between

the orientation process in the retinotopic (vision phase) and action (action phase) representations. (see the supplementary document for all transfer-type classification results).

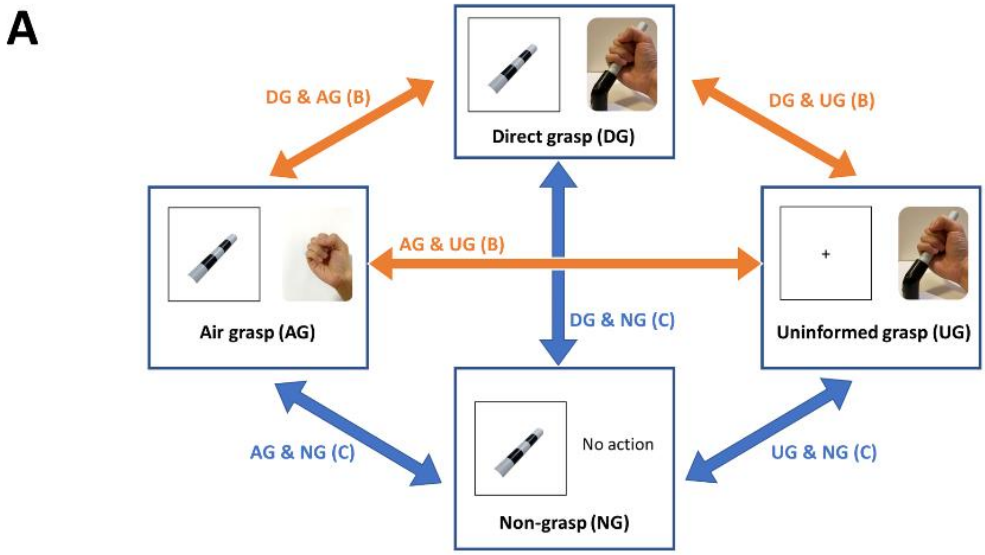

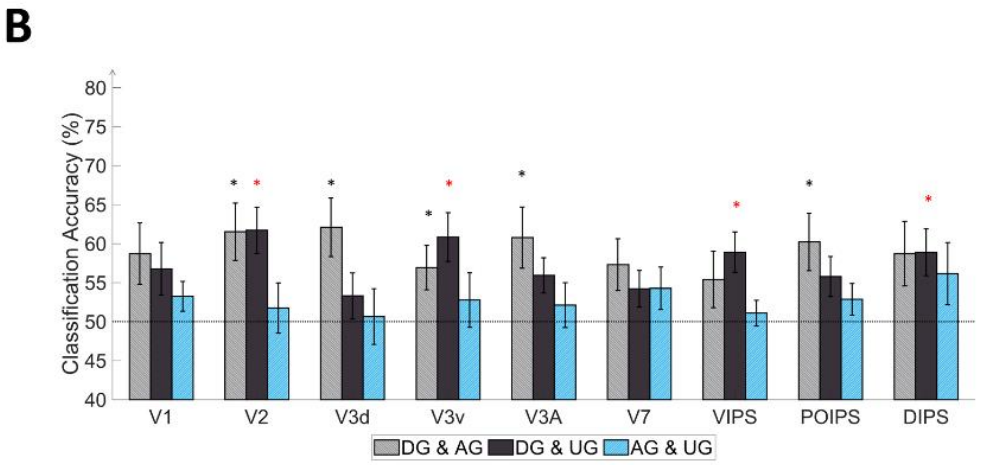

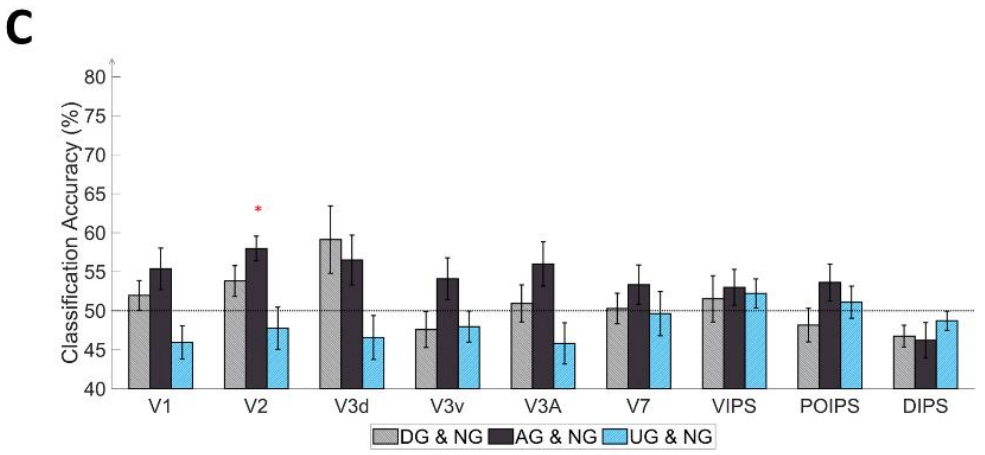

Figure 3.4 Schematics and results of ROI-based MVPA “transfer-type” orientation classification schematics in the action phase. (A) The schematic indicates transfer-type orientation classifications. The transfer-type orientation classification is displayed by arrows pointing to the pair of conditions to transfer as follows: DG & AG, DG & UG, AG & UG, AG & NG, DG & NG, and UN & NG. (B) The bar graph indicates the decoding results from the MVPA classification in the transfer-type classification of the DG & AG, DG & UG, and AG & UG. The areas V2, V3v, VIPS, and DIPS showed significantly high classification accuracy in “DG & UG.” (C) The bar graph displays decoding results from the transfer-type classification of AG & NG, DG & NG, and UN & NG. Only V2 showed significantly high decoding accuracy in “AG & NG.” In every graph, the dashed line indicates the chance level of the classification at 50%. The error bars represent the standard error of the mean across the participants (n = 10). The black asterisk represents the statistical significance over the chance level (50%) or between the grasping types in (2) with two-tailed t-tests across the subjects ($p < 0.05$). The red asterisk indicates the statistical significance based on an FDR correction of $q < 0.05$.

3.6 Discussion

Using fMRI data and the MVPA method, this study aimed to examine the representation of orientation under four non-visually guided action conditions, to understand the factors among the tactile, proprioception, and action-related processes that affect the orientation process in the visual cortices. In the same-type classification (Figure 3.3C), the DG condition demonstrated a high decoding accuracy for V1, V2, V3d, V7, VIPS, POIPS, and DIPS. In the AG condition, significant decoding accuracy was observed in V1, V2, V3v, and V3A. Notably, in the NG condition, in which no action execution took place, although visual instructions were given, the results showed non-significant overall accuracy. This suggests that cortical representation of orientation relies on the action itself in the action phase. Particularly, in the UG condition, the orientation cortical pattern could be decoded from V3d and V3v, which was a surprising result and suggested the involvement of other sources of information from somatosensory and motor systems in the orientation process.

A further distinction of results emerged between DG and AG conditions, particularly in higher dorsal regions (V7 and IPS areas), underscoring the impact of tactile feedback and action-related processes. Alternatively, the cross-decoding results from the V3v and DIPS revealed a shared pattern across the DG-UG condition, whereas the V3d did not exhibit significant transfer decoding. This shared pattern may involve additional cognitive processes, such as visualization of the object during grasping from tactile feedback and proprioception in the visual cortices.

3.6.1 V1 and V2 mainly process orientation from visual information.

Orientation representations in the V1 and V2 areas exhibited a similar tendency, with significantly high decoding accuracy under both the DG and AG conditions (Figure 3.3C). These conditions involved visual object instruction and the execution of the grasping action, with proprioceptive information as a common input. The absence of tactile feedback under the AG condition had a relatively minor impact on the decoded orientation patterns in V1 and V2. This can be attributed to the enhancement of the decoded cortical pattern related to object orientation perception by action planning and execution of the grasping action (Gutteling et al., 2015). Furthermore, V1 and V2 may incorporate a visual working memory component (Harrison and Tong, 2009). Visual information stored in memory can be reactivated during action performance when no real-time visual feedback is available (Singhal et al., 2013; Monaco et al., 2017). Consequently, non-visual information, including tactile feedback, may have less relevance in affecting orientation representation in V1 and V2. In contrast, the NG condition, in which no action occurred, exhibited low decoding accuracy, indicating that the contribution of action-related processes is important to the orientation process in the action phase, especially with no online visual feedback of action. Moreover, the UG condition showed low decoding accuracy in V1 and V2, suggesting that prior information about object orientation is important for the planning and processing orientation during grasping with no real-time visual feedback. Additional results from cross-phase decoding analysis (vision to action and vice versa) revealed a potential inverse-orientation cortical pattern that was correlated across different phases in the DG, AG, and NG conditions. This suggests a distinct representation of visual-related orientation information that was transformed during action execution. Therefore, visual instruction and action execution are both necessary for the cortical pattern of orientation representation in V1 and V2 from evidence in NG and UG results. Overall, our findings suggest that orientation processing in V1 and V2 relies primarily on visually related information evoked by the action process.

3.6.2 Different functional process between V3d and V3v

In the case of the V3 areas, the orientation representation exhibited distinct functional differences between the dorsal and ventral sections. Specifically, V3d displayed reliance on tactile feedback, as evidenced by the significant decoding results under the DG condition and

non-significant results under the AG condition. Previous studies on macaque monkeys emphasize the roles of V3 and VIP in visuotactile integration (Négyessy et al., 2006). Additionally, the V3d is activated during object grasping in the absence of visual stimuli (Kilintari et al., 2011), further supporting the involvement of tactile feedback and action-related processes in this region. Moreover, previous studies have consistently demonstrated selective activation of the lower visual field within the peripersonal space (Previc, 1990; Danckert and Goodale, 2001, 2003), confirming that the V3d area is intricately linked to action-related processes. Our study's characteristic findings in V3d strongly suggested the integration of signals from the somatosensory and motor systems in the representation of orientation during grasping.

Contrarily, V3v, situated in the ventral pathway, is primarily associated with visual recognition processes (Mishkin et al., 1983; Goodale and Milner, 1992). In contrast to V3d, V3v demonstrated significant decoding results under the AG condition, but non-significant results in the DG condition. During grasping in the dark, the activation of the ventral stream area has been observed and is suggested to be related to the visual object recognition process (Singhal et al., 2013). The absence of tactile feedback during object grasping may stimulate visual imagery to compensate for missing information, thereby triggering the visual recognition process, and significantly affecting the decoding accuracy. Furthermore, the visual imagery observed in V3v was action-triggered, which explains the low decoding accuracy observed under the NG condition.

In the UG condition, orientation perception relied solely on uninformed grasping, without visual or memory-related information. Therefore, action planning and the use of memory components for objects were not assumed to be presented. Notably, both V3d and V3v demonstrated significant decoding accuracy under these conditions. In V3d, orientation information is likely utilized for specific action-related processes for each action of the DG and UG, resulting in different orientation patterns when the orientation is not pre-informed in the UG. The action of grasping objects in the dark can activate cortical patterns in the V3d (Kilintari et al., 2011). Moreover, the lower visual field is selectively active for action in the peripersonal space (Previc, 1990; Danckert and Goodale, 2001, 2003), suggesting an action-related process in V3d. The transfer-type classification results for V3d indicate the absence of a shared pattern between the informed (DG) and uninformed (UG) orientation conditions. This suggested a different action process in V3d when an action was not planned.

In V3v, although the DG condition showed non-significant results, the decoding results of the transfer-type classification of the DG and UG were significant. This suggests that the

classifier in the UG condition has a major influence on the cross-decoded results. During grasping, the visual recognition processes in the V3v may involve object visualization and integration of tactile feedback to compensate for missing visual instructions in the UG condition. This notion is supported by studies showing that the ventral visual areas can process object shape recognition, even with partial perception through a narrow slit (Orlov and Zohary, 2018), supporting the object visualization aspect of the V3v in our study. Overall, these findings emphasize the differential orientation processing in the dorsal and ventral pathways within the V3 areas.

3.6.3 Higher dorsal areas representation and contribution of NG condition

In the higher dorsal areas, namely V7, VIPS, POIPS, and DIPS, the representation of orientation appears to rely on tactile feedback, albeit for different reasons compared to V3d, primarily because of the involvement of visuomotor processes (Culham et al., 2003; van Elk et al., 2010). Dorsal pathway areas in the parietal lobe are close to the somatosensory cortex, which receives feedback signals related to motor activity. Notably, a previous study demonstrated the integration of visual and tactile signals of the hand in the anterior IPS in humans (Gentile et al., 2011). During grasping actions, tactile signals may exert a greater influence on the visuomotor processes, particularly when real-time visual feedback is unavailable.

During the action phase, three action conditions activated action-related processes, which are characterized by feedback signals from motor-related areas associated with visuomotor tasks such as grasping (Culham et al., 2003; Petro et al., 2014; Gutteling et al., 2015; Gallivan et al., 2019). In AG and DG conditions, the grasping was planned, while in the UG condition, unplanned grasp was performed. These three conditions showed significant classification accuracy in certain areas. In contrast, the NG condition, where no grasping action was performed, resulted in low classification accuracy across all areas. On the other hand, action planning involves a memory component, specifically working memory (Fiehler et al., 2011; Schenk and Hesse, 2018). Furthermore, a perspective review by van Ede (2020) has proposed that the action modulates visual working memory bidirectionally in visual cortices. These previous studies suggested that in the NG condition, although the object's mental image may have been retained, the memory component does not contribute significantly to the cortical pattern when the grasping action and online visual input are absent.

3.6.4 Limitations

The AG condition in our study had certain limitations that should be acknowledged. Firstly, the difference between the AG condition and other grasping conditions may extend beyond the absence of tactile sensation. The performance of grasping action in the air, without physical contact with an object, may not fully replicate real-world grasping scenarios. In essence, the AG condition represented a form of “pantomime grasping.” Previous investigations comparing pantomime and real grasping tasks have shown that real grasping elicits greater activation in parietal areas (Króliczak et al., 2007), suggesting distinct action processes that could result in the decoding of orientation in our study. Furthermore, attention during the initial stages of grasping an object may affect the grasping action. The DG and UG conditions require careful alignment and shaping of the hand around the object, while the AG condition may involve less attention to this aspect. The less attention to hand position could affect the cortical pattern. Future research on non-visually guided actions should address effective control of tactile feedback presence or absence from objects, as well as ensuring control over the participant's attention during the trials.

The content of visual memory in the NG condition suggested a limitation of this study. Participants had accurately judged orientation in a later phase indicating the retention of instructed orientation in memory despite low decoding accuracy in the action phase. The memory content may take the form of semantics (e.g., left, or right) rather than a visual image of the object, serving as cues for button selection preparation. A recent study by Davis et al. (2021) demonstrated that semantic representations of objects can predict perceptual memory in visual cortices. In particular, semantic representations of the object ("orange") were derived from normatively observed ("is round"), taxonomic ("is a fruit"), and encyclopedic ("is sweet") characteristics. In our study, the low decoding accuracy for "left" or "right" orientation representation suggested a different semantic process for orientation information. To address this limitation, future studies could explore alternative designs or include control conditions to investigate the specific contribution of memory and semantics in orientation processing.

The selection of the ROI may have certain limitations. Initially, our focus was on the early visual and dorsal pathways, given their association with the action process (Culham et al., 2003; Petro et al., 2014). However, our study revealed the involvement of the ventral area V3v in visual recognition processes during orientation representation in grasping tasks without visual feedback. This finding highlights the potential for investigating orientation

processing in higher ventral areas that are responsible for object recognition during action in the absence of visual feedback.

3.7 References of CHAPTER 3

63. Bekkering, H., & Neggers, S. F. (2002). Visual Search Is Modulated by Action Intentions. Psychological Science, 13(4), 370–374. https://doi.org/10.1111/j.0956-7976.2002.00466.x
64. Benjamini, Y., & Yekutieli, D. (2001). The control of the false discovery rate in multiple testing under dependency. The Annals of Statistics, 29(4). https://doi.org/10.1214/aos/1013699998
65. Binkofski, F., Dohle, C., Posse, S., Stephan, K. M., Hefter, H., Seitz, R. J., & Freund, H. J. (1998). Human anterior intraparietal area subserves prehension. Neurology, 50(5), 1253–1259. https://doi.org/10.1212/wnl.50.5.1253.
66. Culham, J. C., Danckert, S. L., Souza, J. F. X. D., Gati, J. S., Menon, R. S., & Goodale, M. A. (2003). Visually guided grasping produces fMRI activation in dorsal but not ventral stream brain areas. Experimental Brain Research, 153(2), 180–189. https://doi.org/10.1007/s00221-003-1591-5
67. Danckert, J. A., & Goodale, M. A., (2001). Superior performance for visually guided pointing in the lower visual field. Experimental Brain Research, 137(3–4), 303–308. https://doi.org/10.1007/s002210000653
68. Danckert, J. A., & Goodale, M. A. (2003). Ups and downs in the visual control of action. In S. H. Johnson-Frey (Ed.), Taking action: Cognitive neuroscience perspectives on intentional acts (pp. 29–64). The MIT Press
69. Davis, S. W., Geib, B. R., Wing, E. A., Wang, W. C., Hovhannisyan, M., Monge, Z. A., & Cabeza, R. (2020). Visual and Semantic Representations Predict Subsequent Memory in Perceptual and Conceptual Memory Tests. Cerebral Cortex, 31(2), 974–992. https://doi.org/10.1093/cercor/bhaa269
70. DeYoe, E. A., Carman, G. J., Bandettini, P., Glickman, S., Wieser, J., Cox, R., . . . Neitz, J. (1996). Mapping striate and extrastriate visual areas in human cerebral cortex. Proceedings of the National Academy of Sciences, 93(6), 2382–2386. https://doi.org/10.1073/pnas.93.6.2382
71. Fabbri, S., Stubbs, K. M., Cusack, R., & Culham, J. C. (2016). Disentangling Representations of Object and Grasp Properties in the Human Brain. Journal of

Neuroscience, 36(29), 7648–7662. https://doi.org/10.1523/jneurosci.0313-16.2016.

72. Faillenot, I. (1997). Visual pathways for object-oriented action and object recognition: functional anatomy with PET. Cerebral Cortex, 7(1), 77–85. https://doi.org/10.1093/cercor/7.1.77
73. Fiehler, K., Bannert, M. M., Bischoff, M., Blecker, C., Stark, R., Vaitl, D., Franz, V. H., & Rösler, F. (2011). Working memory maintenance of grasp-target information in the human posterior parietal cortex. NeuroImage, 54(3), 2401–2411. https://doi.org/10.1016/j.neuroimage.2010.09.080
74. Fischl, B. (2012). FreeSurfer. NeuroImage, 62(2), 774–781. https://doi.org/10.1016/j.neuroimage.2012.01.021
75. Gallivan, J. P., Chapman, C. S., Gale, D. J., Flanagan, J. R., & Culham, J. C. (2019). Selective Modulation of Early Visual Cortical Activity by Movement Intention. Cerebral Cortex, 29(11), 4662–4678. https://doi.org/10.1093/cercor/bhy345
76. Gentile, G., Petkova, V. I., & Ehrsson, H. H. (2011). Integration of visual and tactile signals from the hand in the human brain: an FMRI study. Journal of neurophysiology, 105(2), 910–922. https://doi.org/10.1152/jn.00840.2010
77. Goodale, M. A., & Milner, A. (1992). Separate visual pathways for perception and action. Trends in Neurosciences, 15(1), 20–25. https://doi.org/10.1016/0166-2236(92)90344-8
78. Gutteling, T. P., Kenemans, J. L., & Neggers, S. F. W. (2011). Grasping Preparation Enhances Orientation Change Detection. PLoS ONE, 6(3), e17675. https://doi.org/10.1371/journal.pone.0017675
79. Gutteling, T. P., Petridou, N., Dumoulin, S. O., Harvey, B. M., Aarnoutse, E. J., Kenemans, J. L., & Neggers, S. F. (2015). Action Preparation Shapes Processing in Early Visual Cortex. The Journal of Neuroscience, 35(16), 6472–6480. https://doi.org/10.1523/jneurosci.1358-14.2015
80. Harrison, S. A., & Tong, F. (2009). Decoding reveals the contents of visual working memory in early visual areas. Nature, 458(7238), 632–635. https://doi.org/10.1038/nature07832
81. Kilintari, M., Raos, V., & Savaki, H. E. (2011). Grasping in the Dark Activates Early Visual Cortices. Cerebral Cortex, 21(4), 949–963. https://doi.org/10.1093/cercor/bhq175
82. Króliczak, G., Cavina-Pratesi, C., Goodman, D. A., & Culham, J. C. (2007). What does the brain do when you fake it? An FMRI study of pantomimed and real grasping.

Journal of neurophysiology, 97(3), 2410–2422. https://doi.org/10.1152/jn.00778.2006

83. Marangon, M., Kubiak, A., & Króliczak, G. (2016). Haptically Guided Grasping. fMRI Shows Right-Hemisphere Parietal Stimulus Encoding, and Bilateral Dorso-Ventral Parietal Gradients of Object- and Action-Related Processing during Grasp Execution. Frontiers in Human Neuroscience, 9. https://doi.org/10.3389/fnhum.2015.00691
84. Mishkin, M., Ungerleider, L. G., & Macko, K. A. (1983). Object vision and spatial vision: two cortical pathways. Trends in Neurosciences, 6, 414–417. https://doi.org/10.1016/0166-2236(83)90190-x
85. Monaco, S., Cavina-Pratesi, C., Sedda, A., Fattori, P., Galletti, C., & Culham, J. C. (2011). Functional magnetic resonance adaptation reveals the involvement of the dorsomedial stream in hand orientation for grasping. Journal of Neurophysiology, 106(5), 2248–2263. https://doi.org/10.1152/jn.01069.2010
86. Monaco, S., Gallivan, J. P., Figley, T. D., Singhal, A., & Culham, J. C. (2017). Recruitment of Foveal Retinotopic Cortex During Haptic Exploration of Shapes and Actions in the Dark. The Journal of Neuroscience, 37(48), 11572–11591. https://doi.org/10.1523/jneurosci.2428-16.2017
87. Monaco, S., Malfatti, G., Culham, J. C., Cattaneo, L., & Turella, L. (2020). Decoding motor imagery and action planning in the early visual cortex: Overlapping but distinct neural mechanisms. NeuroImage, 218, 116981. https://doi.org/10.1016/j.neuroimage.2020.116981
88. Murata, A., Gallese, V., Luppino, G., Kaseda, M., & Sakata, H. (2000). Selectivity for the Shape, Size, and Orientation of Objects for Grasping in Neurons of Monkey Parietal Area AIP. Journal of Neurophysiology, 83(5), 2580–2601. https://doi.org/10.1152/jn.2000.83.5.2580
89. Négyessy, L., Nepusz, T., Kocsis, L. and Bazsó, F. (2006), Prediction of the main cortical areas and connections involved in the tactile function of the visual cortex by network analysis. European Journal of Neuroscience, 23: 1919-1930. https://doi.org/10.1111/j.1460-9568.2006.04678.x
90. Orban, G. A. (2016). Functional definitions of parietal areas in human and non-human primates. Proceedings of the Royal Society B: Biological Sciences, 283(1828), 20160118
91. Orlov, T., & Zohary, E. (2018). Object Representations in Human Visual Cortex Formed Through Temporal Integration of Dynamic Partial Shape Views. The Journal of neuroscience : the official journal of the Society for Neuroscience, 38(3), 659–678.

https://doi.org/10.1523/JNEUROSCI.1318-17.2017

92. Petro, L. S., Vizioli, L., & Muckli, L. (2014). Contributions of cortical feedback to sensory processing in primary visual cortex. Frontiers in Psychology, 5. https://doi.org/10.3389/fpsyg.2014.01223
93. Previc, F. H. (1990). Functional specialization in the lower and upper visual fields in humans: Its ecological origins and neurophysiological implications. Behavioral and Brain Sciences, 13(3), 519–542. https://doi.org/10.1017/s0140525x00080018
94. Sathian, K., & Zangaladze, A. (2002). Feeling with the mind's eye: contribution of visual cortex to tactile perception. Behavioural Brain Research, 135(1–2), 127–132. https://doi.org/10.1016/s0166-4328(02)00141-9
95. Schenk, T., & Hesse, C. (2018). Do we have distinct systems for immediate and delayed actions? A selective review on the role of visual memory in action. Cortex; a journal devoted to the study of the nervous system and behavior, 98, 228–248. https://doi.org/10.1016/j.cortex.2017.05.014
96. Sereno, M. I., Dale, A. M., Reppas, J. B., Kwong, K. K., Belliveau, J. W., Brady, T. J., Rosen, B. R., & Tootell, R. B. (1995). Borders of multiple visual areas in humans revealed by functional magnetic resonance imaging. Science (New York, N.Y.), 268(5212), 889–893. https://doi.org/10.1126/science.7754376
97. Singhal, A., Monaco, S., Kaufman, L. D., & Culham, J. C. (2013). Human fMRI Reveals That Delayed Action Re-Recruits Visual Perception. PLoS ONE, 8(9), e73629. https://doi.org/10.1371/journal.pone.0073629
98. Smith, M. A., & Soechting, J. F. (2005). Modulation of grasping forces during object transport. Journal of neurophysiology, 93(1), 137–145. https://doi.org/10.1152/jn.00775.2004
99. van der Groen, O., van der Burg, E., Lunghi, C., & Alais, D. (2013). Touch influences visual perception with a tight orientation-tuning. PloS one, 8(11), e79558. https://doi.org/10.1371/journal.pone.0079558
100. van Ede F. (2020). Visual working memory and action: Functional links and bi-directional influences. Visual cognition, 28(5-8), 401–413. https://doi.org/10.1080/13506285.2020.1759744
101. van Elk, M., van Schie, H. T., Neggers, S. F., & Bekkering, H. (2010). Neural and temporal dynamics underlying visual selection for action. Journal of neurophysiology, 104(2), 972–983. https://doi.org/10.1152/jn.01079.2009
102. Vanduffel, W., Fize, D., Peuskens, H., Denys, K., Sunaert, S., Todd, J. T., & Orban, G.

A. (2002). Extracting 3D from motion: differences in human and monkey intraparietal cortex. Science (New York, N.Y.), 298(5592), 413–415. https://doi.org/10.1126/science.1073574

103. Velji‐Ibrahim, J., Crawford, J. D., Cattaneo, L., & Monaco, S. (2022). Action planning modulates the representation of object features in human fronto‐parietal and occipital cortex. European Journal of Neuroscience, 56(6), 4803‐4818. https://doi.org/10.1111/ejn.15776
104. Warnking, J., Dojat, M., Guérin-Dugué, A., Delon-Martin, C., Olympieff, S., Richard, N., Chéhikian, A., & Segebarth, C. (2002). fMRI retinotopic mapping--step by step. NeuroImage, 17(4), 1665–1683. https://doi.org/10.1006/nimg.2002.1304
105. Zangaladze, A., Epstein, C. M., Grafton, S. T., & Sathian, K. (1999). Involvement of visual cortex in tactile discrimination of orientation. Nature, 401(6753), 587–590. https://doi.org/10.1038/44139

CHAPTER 4

Conclusion

In the first topic, we decoded the orientation representation during different types of visually occluded action in human visual cortices. The early visual areas V1, V2 processes orientation in vision-related information from the object in occluded action, which is independent of action types. V3d showed decoded orientation representation for each action type but did not convey a generalized representation in occluded action. This suggests that, in V3d, each action may be selective causing the specific cortical pattern. In the higher dorsal area, the orientation representation tends to be action specific when performs occluded actions. However, ventral areas known for visual recognition showed no orientation representation with or without visual input. This suggests that without visual input, a grasping action can modulate the orientation representation in human visual cortices; particularly, V3d suggests the involvement and unique representations in precise and full grasping types. Hence, our data can serve as groundwork for examining orientation processing using an action without online visual guidance.

In the second topic, our study revealed that non-visual information, including tactile feedback, proprioceptive information, and action-related processes, plays a significant role in orientation representation within the human visual cortex. Orientation representation within the V1 and V2 exhibited a strong dependence on both the visual information and the action process. In the V3 areas, the findings highlighted differential processing in the dorsal and ventral sections of V3, where tactile feedback influenced orientation perception in V3d for the specific action-related process, while visual imagery of the object compensated for the absence of object information in V3v. These findings provide valuable insights into the complex interplay between sensory inputs and motor-related processes, and their impact on orientation perception, highlighting the variability among different areas within the human visual cortex.

Appendix

Table A.1: Univariate results value of vision phase in research topic 1#

ROI	Vision phase					
	Full grasp vs baseline			Precise grasp vs baseline		
	Signal changes (%)	Error	p-values	Signal changes (%)	Error	p-values
V1	0.965934	0.062444	2.06E-07	0.978087	0.082746	2.04E-06
V2	0.861775	0.057529	2.72E-07	0.847371	0.08791	1.11E-05
V3d	0.78797	0.078365	7.83E-06	0.754051	0.083906	1.95E-05
V3v	0.948619	0.089629	5.14E-06	0.871413	0.073735	2.05E-06
V3A	0.746435	0.05923	1.19E-06	0.706727	0.059591	1.99E-06
V7	0.693588	0.047769	3.56E-07	0.682872	0.052244	8.74E-07
KO	0.777705	0.074389	5.69E-06	0.740184	0.07112	5.9E-06
hMT+	0.675327	0.041708	1.39E-07	0.669313	0.04949	6.54E-07
LOC	0.674966	0.057125	2.05E-06	0.670113	0.052404	1.05E-06
VIPS	0.683602	0.053161	1E-06	0.671172	0.060951	3.7E-06
POIPS	0.653432	0.063773	6.71E-06	0.665835	0.068915	1.09E-05
DIPS	0.557127	0.04008	5.17E-07	0.560894	0.044501	1.19E-06

Table A.2: Univariate results value of action phase in research topic 1#

ROI	Action phase					
	Full grasp vs baseline			Precise grasp vs baseline		
	Signal changes (%)	Error	p-values	Signal changes (%)	Error	p-values
V1	0.981445	0.08636	2.84E-06	1.011824	0.08747	2.45E-06
V2	0.822748	0.065548	1.23E-06	0.83911	0.072122	2.34E-06
V3d	0.664795	0.068195	1.01E-05	0.690437	0.068463	7.65E-06
V3v	0.929353	0.114164	4.27E-05	0.917986	0.082959	3.55E-06
V3A	0.676537	0.056412	1.81E-06	0.711416	0.056127	1.13E-06
V7	0.651355	0.041182	1.7E-07	0.679883	0.043665	1.95E-07
KO	0.68291	0.060478	3E-06	0.724776	0.06944	5.76E-06
hMT+	0.805643	0.047253	8.86E-08	0.812421	0.059886	6.36E-07
LOC	0.646203	0.042538	2.41E-07	0.666459	0.064663	6.39E-06
VIPS	0.647804	0.045408	4.14E-07	0.673052	0.054356	1.38E-06
POIPS	0.671497	0.06045	3.44E-06	0.673868	0.060053	3.16E-06
DIPS	0.673497	0.04398	2.25E-07	0.683468	0.044024	2E-07

Table A.3: MVPA results of the control session in research topic 1#

ROI	2D orientation classification				3D orientation classification			
	Vision phase		Judgment phase		Vision phase		Judgment phase	
	Accuracy (%)	Corrected p	Accuracy (%)	Corrected p	Accuracy (%)	Corrected p	Accuracy (%)	Corrected p
V1	64.65923	**0.01833**	50.125	0.940765	50.51116	0.957777	48.19196	0.502025
V2	66.90997	**0.016874**	53.91369	**0.044841**	52.22545	0.957777	50.59821	0.818378
V3d	65.02232	**0.016874**	53.94717	**0.044841**	50.85119	0.957777	52.61384	0.356352
V3v	54.48214	0.094586	50.87277	0.664274	51.16964	0.957777	55.95536	0.282821
V3A	57.74851	**0.030069**	52.21057	0.252343	46.99554	0.957777	51.53869	0.365722
V7	56.13765	**0.030069**	54.74851	**0.019608**	50.70536	0.957777	52.27083	0.367967
KO	58.75	**0.016874**	55.46801	**0.044841**	48.45759	0.957777	52.62128	0.282821
hMT+	54.40327	**0.017988**	51.52009	0.230831	51.0439	0.957777	50.3936	0.818378
LOC	51.87946	0.316898	52.47917	0.185019	49.93452	0.957777	48.44866	0.502025
VIPS	50.56771	0.782962	53.06845	0.230831	49.75521	0.957777	48.86756	0.818378
POIPS	49.27827	0.506222	51.40699	**0.11378**	50.1369	0.957777	52.00893	0.367967
DIPS	50.76711	0.782962	53.9308	0.230831	49.3192	0.957777	52.83185	0.287309

Table A.4: Post hoc analysis of Table A3 results

ROIs	2D orientation classification				3D orientation classification			
	Vision phase		Judgment phase		Vision phase		Judgment phase	
	Effect size	Power (1 - β err prob)	Effect size	Power (1 - β err prob)	Effect size	Power (1 - β err prob)	Effect size	Power (1 - β err prob)
V1	1.13973	0.8926	0.0102	0.0506	0.1046	0.06016	0.3101	0.1422
V2	1.2666	0.9442	1.0493	0.8389	0.3942	0.20057	0.1025	0.0598
V3d	1.35306	0.9664	1.0001	0.8032	0.1516	0.07149	0.5747	0.3689
V3v	0.7066	0.5138	0.1767	0.0793	0.175	0.07871	0.89	0.7077
V3A	0.96731	0.7769	0.4497	0.2467	0.448	0.24519	0.5212	0.3139
V7	0.9732	0.7818	1.4785	0.9852	0.1109	0.06145	0.445	0.2426
KO	1.27642	0.9472	1.1055	0.874	0.2653	0.11698	0.7661	0.5796
MT+	1.191	0.9166	0.4932	0.2866	0.266	0.11736	0.0788	0.0558
LOC	0.42164	0.2227	0.6273	0.4257	0.0181	0.0503	0.3355	0.1583
VIPS	0.09461	0.0583	0.5405	0.3334	0.0681	0.0543	0.1291	0.0655
POIPS	0.28051	0.1251	0.7649	0.5783	0.0352	0.05115	0.4665	0.2618
DIPS	0.10917	0.0611	0.5168	0.3096	0.1287	0.06545	0.6798	0.4839

Table A.5: MVPA results of the 2D orientation classification from grasping session in research topic 1#

ROI	Vision phase				Action phase			
	Precise grasp		Full grasp		Precise grasp		Full grasp	
	Accuracy (%)	Corrected p	Accuracy (%)	Corrected p	Accuracy (%)	Corrected p	Accuracy (%)	Corrected p
V1	65.625	**0.006451**	60.1875	0.066298	56.3125	0.159856	61.75	**0.025849**
V2	63.375	**0.006451**	61.3125	**0.006274**	55.96875	0.159856	61.53125	0.050952
V3d	65.4375	**0.000792**	63.625	**0.008939**	60.84375	**0.007227**	63.5	**0.00917**
V3v	56.6875	0.281469	53.40625	0.512331	53.9375	0.159856	57.5625	0.117684
V3A	53.71875	0.442834	53.46875	0.258026	54.03125	0.241383	62.625	**0.010747**
V7	49.375	0.783974	52.1875	0.468324	53.0625	0.241383	59.21875	0.053379
KO	52.5625	0.442834	52.59375	0.512331	52.9375	0.175555	56.53125	0.142676
hMT+	52.03125	0.442834	47.0625	0.468324	55.84375	0.060535	59.53125	0.110885
LOC	54.65625	0.281469	45.84375	0.113108	54.25	0.123395	59.3125	0.082096
VIPS	51.28125	0.770686	51.625	0.556955	50.125	0.964021	60.5	**0.010747**
POIPS	48.625	0.770686	50.09375	1	54.75	0.159856	58.9375	0.110885
DIPS	51.15625	0.770686	50	1	54	0.159856	64.21875	**0.00917**

Table A.6: Post hoc analysis of Table A5 results

ROIs	Vision phase				Action phase			
	Precise grasp		Full grasp		Precise grasp		Full grasp	
	Effect size	Power (1 - β err prob)	Effect size	Power (1 - β err prob)	Effect size	Power (1 - β err prob)	Effect size	Power (1 - β err prob)
V1	1.518082	0.988822	0.978913	0.786435	0.597654	0.393388	1.067837	0.851091
V2	1.481546	0.985513	1.752333	0.998285	0.599076	0.394921	0.891167	0.708799
V3d	2.3204	0.999996	1.49985	0.987263	1.717044	0.997671	1.49396	0.986721
V3v	0.577401	0.371737	0.304868	0.139023	0.679307	0.483325	0.595085	0.390622
V3A	0.370451	0.182659	0.595802	0.391393	0.438084	0.2366	1.302251	0.954475
V7	0.094155	0.058232	0.389009	0.196584	0.441209	0.239298	0.85037	0.668638
KO	0.37898	0.188975	0.312196	0.143461	0.552712	0.345887	0.535424	0.328198
MT+	0.404633	0.208829	0.421461	0.222539	1.081431	0.859671	0.637043	0.436382
LOC	0.583042	0.37773	0.811504	0.628437	0.852267	0.670555	0.735598	0.546041
VIPS	0.159872	0.073917	0.254841	0.111695	0.01546	0.050221	1.337977	0.963149
POIPS	0.1296	0.065655	0.01934	0.050346	0.628249	0.426701	0.627573	0.425958
DIPS	0.137794	0.067715	0	0.05	0.598	0.393761	1.501356	0.987399

Table A.7: MVPA results of the 3D orientation classification from grasping session in research topic 1#

ROI	Vision phase				Action phase			
	Precise grasp		Full grasp		Precise grasp		Full grasp	
	Accuracy (%)	p	Accuracy (%)	p	Accuracy (%)	p	Accuracy (%)	p
V1	52.75	0.286088	45.15625	**0.031376**	55.8125	0.087597	50.40625	0.811739
V2	47.90625	0.248698	49.15625	0.74728	53.53125	0.378265	53.71875	**0.036814**
V3d	49.90625	0.960144	50	1	53.9375	0.327849	52.6875	0.241096
V3v	49.03125	0.328104	50.875	0.723673	55.125	0.103163	53.84375	0.080183
V3A	48.3125	0.342737	48.875	0.712061	53.09375	0.242342	55.0625	0.065153
V7	45.03125	0.052477	46.9375	0.301725	50.6875	0.843585	49.6875	0.873201
KO	54.875	0.108768	49.625	0.870127	52.53125	0.355526	56.625	**0.020495**
hMT+	47.0625	0.263167	45.4375	0.060497	50.625	0.860336	53	0.374452
LOC	49.875	0.890227	52.03125	0.457238	54.21875	0.088652	52.5	0.410371
VIPS	50.40625	0.828776	51.8125	0.452285	50.34375	0.911811	54.75	0.139693
POIPS	47.5	0.288045	48.3125	0.605718	50.8125	0.667836	58.75	**0.001452**
DIPS	49.71875	0.932547	49	0.695672	50.75	0.700585	57.4375	**0.020546**

Table A.8: Post hoc analysis of Table A7 results

ROIs	Vision phase				Action phase			
	Precise grasp		Full grasp		Precise grasp		Full grasp	
	Effect size	Power (1 - β err prob)	Effect size	Power (1 - β err prob)	Effect size	Power (1 - β err prob)	Effect size	Power (1 - β err prob)
V1	0.378006	0.188246	0.848821	0.66707	0.638712	0.438223	0.081761	0.0562
V2	0.411105	0.214038	0.110763	0.06141	0.308899	0.14145	0.816353	0.633542
V3d	0.017127	0.050271	0	0.05	0.34487	0.164595	0.418324	0.219943
V3v	0.344679	0.164465	0.121606	0.06377	0.604496	0.40078	0.657078	0.458568
V3A	0.333843	0.157217	0.126991	0.065026	0.417128	0.218958	0.69989	0.506299
V7	0.744186	0.55554	0.365184	0.178832	0.067695	0.054246	0.054734	0.052774
KO	0.593349	0.388756	0.056075	0.052911	0.324653	0.151259	0.935492	0.749628
MT+	0.397848	0.203453	0.715102	0.523264	0.060352	0.053373	0.311491	0.143029
LOC	0.047325	0.052073	0.258915	0.113727	0.636219	0.435473	0.287777	0.129104
VIPS	0.074218	0.055106	0.261868	0.115221	0.03797	0.051334	0.539986	0.332831
POIPS	0.376372	0.187028	0.178281	0.079822	0.147851	0.070422	1.505725	0.987785
DIPS	0.029013	0.050778	0.134654	0.06691	0.132349	0.066331	0.934981	0.749175

Table A.9: MVPA results of the transfer-type orientation classification from grasping session in research topic 1#

ROI	2D orientation classification				3D orientation classification			
	Vision phase		Action phase		Vision phase		Action phase	
	Accuracy (%)	Corrected p	Accuracy (%)	Corrected p	Accuracy (%)	p	Accuracy (%)	p
V1	60.21875	0.018611	57.875	0.042129	51.04688	0.530323	49.70313	0.89784
V2	61.51563	0.018611	58.53125	0.024152	49.79688	0.890056	47.42188	0.289047
V3d	61.85938	0.01653	54.84375	0.15113	50.48438	0.792264	48.92188	0.559798
V3v	53.03125	0.421338	56.29688	0.024152	47.75	0.189936	49.5625	0.771295
V3A	54.89063	0.09865	54.75	0.042129	52.70313	0.101744	52.14063	0.194833
V7	51.75	0.474941	53.15625	0.148272	51.95313	0.177268	52.5625	0.09483
KO	55.375	0.084025	54.21875	0.061375	49	0.441245	48.29688	0.366862
hMT+	51.4375	0.263957	53.375	0.22649	46.625	0.115179	45.04688	0.014407
LOC	52.85938	0.164678	55.0625	0.025166	49.76563	0.916388	50.4375	0.880275
VIPS	49.10938	0.611493	53.35938	0.090136	49.9375	0.976559	50.75	0.698699
POIPS	52.26563	0.421338	55.25	0.024152	50.03125	0.979115	49.04688	0.703272
DIPS	49.26563	0.46984	55.03125	0.042129	49.78125	0.900054	47.45313	0.205148

Table A.10: Post hoc analysis of Table A9 results

ROIs	2D orientation classification				3D orientation classification			
	Vision phase		Action phase		Vision phase		Action phase	
	Effect size	Power (1 - β err prob)	Effect size	Power (1 - β err prob)	Effect size	Power (1 - β err prob)	Effect size	Power (1 - β err prob)
V1	1.29857	0.953495	0.909647	0.726199	0.217536	0.094677	0.044021	0.051793
V2	1.2454	0.937345	1.291665	0.951609	0.0474	0.052079	0.375539	0.186409
V3d	1.518094	0.988823	0.541779	0.334659	0.090441	0.057592	0.201836	0.088363
V3v	0.35392	0.170835	1.189515	0.915946	0.472591	0.267349	0.099863	0.059265
V3A	0.793943	0.609759	0.938415	0.752207	0.607407	0.403936	0.466892	0.262131
V7	0.272124	0.120551	0.5663	0.360034	0.48795	0.281676	0.622159	0.42002
KO	0.871895	0.690114	0.794874	0.610756	0.268529	0.118658	0.316709	0.14625
MT+	0.518889	0.311634	0.432742	0.232026	0.581234	0.375806	1.007691	0.80897
LOC	0.651576	0.45246	1.120015	0.882155	0.03599	0.051198	0.051652	0.05247
VIPS	0.175388	0.07885	0.692307	0.497834	0.01007	0.050094	0.133233	0.066552
POIPS	0.369368	0.181868	1.257589	0.941389	0.004298	0.050017	0.131091	0.06602
DIPS	0.300021	0.136149	0.898488	0.715755	0.043061	0.051716	0.455277	0.251664

Table A.11: Left hemisphere MVPA results of the 2D orientation classification from grasping session in research topic 1#

ROI	Vision phase				Action phase			
	Precise grasp		Full grasp		Precise grasp		Full grasp	
	Accuracy (%)	Corrected p	Accuracy (%)	Corrected p	Accuracy (%)	Corrected p	Accuracy (%)	Corrected p
V1	61.5	0.018773	60.34375	0.173572	55.5	0.095556	59.25	0.062073
V2	63.71875	0.018773	56.6875	0.43603	57.90625	0.090085	60.28125	0.035531
V3d	59.3125	0.008519	56.53125	0.43603	59.71875	0.090405	61.5625	0.02819
V3v	56.40625	0.041546	54.5	0.481565	53.53125	0.225204	58.25	0.129221
V3A	53.625	0.462029	53.71875	0.481565	55.4375	0.090085	60.8125	0.031725
V7	48.625	0.606837	50.75	0.757842	51.625	0.509586	56.6875	0.058282
KO	51.09375	0.606837	50.5	0.757842	53.15625	0.256129	55.375	0.12061
hMT+	52.09375	0.606837	49.1875	0.757842	52.21875	0.44889	59.21875	0.062073
LOC	53.46875	0.606837	50.90625	0.757842	51.8125	0.447679	60.03125	0.058282
VIPS	50.1875	0.926112	48.375	0.43603	51.34375	0.513914	59.90625	0.012799
POIPS	53.53125	0.504477	52.09375	0.704796	53.78125	0.225204	58.03125	0.062073
DIPS	51.75	0.606837	46.71875	0.515227	51.9375	0.447679	63.125	0.012799

Table A.12: Post hoc analysis of Table A11 results

ROIs	Vision phase				Action phase			
	Precise grasp		Full grasp		Precise grasp		Full grasp	
	Effect size	Power (1 - β err prob)	Effect size	Power (1 - β err prob)	Effect size	Power (1 - β err prob)	Effect size	Power (1 - β err prob)
V1	1.243527	0.936704	1.006879	0.808356	0.845763	0.663964	0.747122	0.558781
V2	1.326478	0.960519	0.531418	0.324153	1.11075	0.877006	1.002095	0.804707
V3d	1.676487	0.996724	0.623758	0.421772	0.915542	0.731638	1.156702	0.901035
V3v	1.015835	0.815071	0.418626	0.220192	0.586027	0.380914	0.556729	0.350049
V3A	0.469578	0.264583	0.423788	0.224477	0.999208	0.802486	1.071644	0.853529
V7	0.22624	0.098393	0.118263	0.063018	0.253084	0.11083	0.837549	0.655568
KO	0.203692	0.089083	0.105953	0.060436	0.525436	0.318149	0.5899	0.385056
MT+	0.245798	0.107308	0.170244	0.077162	0.311749	0.143187	0.752598	0.564813
LOC	0.323918	0.150791	0.145604	0.0698	0.342149	0.162751	0.83252	0.650387
VIPS	0.031789	0.050935	0.535315	0.328088	0.226501	0.098506	1.417653	0.97768
POIPS	0.407804	0.211371	0.25148	0.110045	0.594044	0.389503	0.753795	0.566131
DIPS	0.236931	0.103169	0.366129	0.179515	0.338965	0.160613	1.460307	0.983224

Table A.13: Right hemisphere MVPA results of the 2D orientation classification from grasping session in research topic 1#

ROI	Vision phase				Action phase			
	Precise grasp		Full grasp		Precise grasp		Full grasp	
	Accuracy (%)	Corrected p	Accuracy (%)	Corrected p	Accuracy (%)	Corrected p	Accuracy (%)	Corrected p
V1	60.75	0.105814	56.59375	0.230274	51.59375	0.982838	60.15625	0.040393
V2	58.84375	0.105814	59.3125	0.177385	50	1	63.71875	0.007577
V3d	61.21875	0.002296	55.46875	0.165182	55.03125	0.421813	60.3125	0.012031
V3v	52.125	0.684197	54.375	0.230274	49.375	0.982838	59.1875	0.040393
V3A	50.3125	0.895789	53.125	0.177385	51.9375	0.873513	58.3125	0.040393
V7	52.78125	0.397125	50.46875	0.847083	51.9375	0.873513	58.09375	0.071845
KO	54.5	0.200166	51.375	0.539966	50.3125	0.982838	59.40625	0.018669
hMT+	50.71875	0.813553	51.65625	0.539966	52.96875	0.837623	59.9375	0.040393
LOC	52.03125	0.541243	46.90625	0.399899	53.59375	0.837623	58.78125	0.040393
VIPS	54.78125	0.115107	49.625	0.847083	50.28125	0.982838	60.96875	0.007577
POIPS	46.8125	0.431539	47.3125	0.399899	54.5	0.421813	59.125	0.051748
DIPS	49.3125	0.818461	51.5625	0.559139	56.15625	0.421813	61.5625	0.040393

Table A.14: Post hoc analysis of Table A13 results

ROIs	Vision phase				Action phase			
	Precise grasp		Full grasp		Precise grasp		Full grasp	
	Effect size	Power (1 - β err prob)	Effect size	Power (1 - β err prob)	Effect size	Power (1 - β err prob)	Effect size	Power (1 - β err prob)
V1	0.890093	0.707772	0.619707	0.417337	0.151429	0.071433	0.933827	0.748151
V2	0.883508	0.701437	0.822351	0.639825	0	0.05	1.53842	0.990361
V3d	2.015423	0.999866	1.017081	0.815993	0.651182	0.452023	1.340755	0.963763
V3v	0.226924	0.098691	0.62361	0.421609	0.079821	0.055909	0.885141	0.703014
V3A	0.04491	0.051866	0.778499	0.593111	0.228915	0.099566	0.836395	0.654381
V7	0.462633	0.258266	0.066159	0.054055	0.261355	0.11496	0.679771	0.483843
KO	0.648912	0.449507	0.291244	0.131067	0.042679	0.051685	1.183088	0.913167
MT+	0.143023	0.069098	0.295078	0.133267	0.329304	0.154253	0.834545	0.652476
LOC	0.404195	0.208479	0.427819	0.227857	0.37823	0.188413	0.900618	0.717763
VIPS	0.807942	0.624672	0.082308	0.056284	0.042689	0.051686	1.608654	0.994343
POIPS	0.408275	0.21175	0.425951	0.226287	0.599875	0.395783	0.764786	0.578182
DIPS	0.109405	0.061131	0.253771	0.111168	0.685115	0.489806	0.856583	0.674899

Table A.15: Orientation Judgement scores from Control session in research topic 1#

Run	P1 score	P2 score	P3 score	P4 score	P5 score	P6 score	P7 score	P8 score	P9 score	P10 score
1	16	16	16	16	16	15	16	15	16	16
2	16	16	16	16	16	16	16	16	16	16
3	16	16	16	16	13	16	15	16	16	14
4	16	16	16	15	16	14	14	16	16	14
5	16	16	16	16	16	13	15	16	16	15
6	16	16	16	15	15	16	16	16	16	16
7	16	16	16	16	16	16	16	16	16	16
8	16	16	16	15	16	16	16	16	16	16
9	16	16	16	15	16	16	16	16	16	16
10	16	16	16	16	16	16	16	16	16	14
Summary	160	160	160	156	156	154	156	159	160	153
% scores	100	100	100	97.5	97.5	96.25	97.5	99.375	100	95.625

Table A.16: Univariate results value of figure 2.2B in research topic 2#

ROI	Instruction phase			Action phase			Judgment phase		
	Signal changes (%)	**standard error**	**p**	**Signal changes (%)**	**standard error**	**p**	**Signal changes (%)**	**standard error**	**p**
V1	0.9548	0.0490	**3E-08**	0.8567	0.0773	**4E-06**	0.9491	0.0550	**8E-08**
V2	0.8652	0.0686	**1E-06**	0.7842	0.0704	**3E-06**	0.8412	0.0580	**4E-07**
V3d	0.8173	0.0704	**2E-06**	0.6588	0.0708	**1E-05**	0.7593	0.0767	**9E-06**
V3v	0.8072	0.0807	**8E-06**	0.7606	0.0567	**7E-07**	0.7700	0.0881	**2E-05**
V3A	0.7223	0.0622	**2E-06**	0.6556	0.0602	**4E-06**	0.7564	0.0582	**9E-07**
V7	0.6837	0.0519	**8E-07**	0.6012	0.0404	**3E-07**	0.6178	0.0629	**9E-06**
VIPS	0.6453	0.0599	**4E-06**	0.6201	0.0418	**3E-07**	0.6761	0.0631	**5E-06**
POIPS	0.6025	0.0603	**8E-06**	0.6176	0.0495	**1E-06**	0.6558	0.0519	**1E-06**
DIPS	0.5078	0.0387	**9E-07**	0.6608	0.0414	**2E-07**	0.5822	0.0663	**2E-05**

Table A.17: Univariate results value of figure 2.2C in research topic 2#

ROI	UG instruction vs baseline			NG action vs baseline		
	Signal changes (%)	**standard error**	**p**	**Signal changes (%)**	**standard error**	**p**
V1	0.4551	0.0345	**8E-07**	0.4767	0.0351	**6E-07**
V2	0.4499	0.0133	**2E-10**	0.4217	0.0435	**1E-05**
V3d	0.4655	0.0448	**6E-06**	0.3677	0.0336	**4E-06**
V3v	0.3942	0.0232	**9E-08**	0.4059	0.0440	**2E-05**
V3A	0.3621	0.0213	**9E-08**	0.3939	0.0376	**6E-06**
V7	0.4060	0.0184	**9E-09**	0.3547	0.0205	**8E-08**
VIPS	0.3492	0.0119	**7E-10**	0.3590	0.0599	**4E-04**
POIPS	0.4178	0.0109	**7E-11**	0.3603	0.0383	**1E-05**
DIPS	0.2409	0.0350	**2E-04**	0.2292	0.0505	0.003

Table A.18: MVPA results of the Instruction phase in research topic 2#

ROIs	DG			AG			NG			UG		
	Accuracy (%)	**p**	**q**	**Accuracy (%)**	**p**	**q**	**Accuracy (%)**	**p**	**q**	**Accuracy (%)**	**p**	**q**
V1	66.44	**0.003**	**0.015**	68.31	**1E-04**	**0.001**	65.25	**0.016**	**0.049**	47.75	0.572	0.644
V2	70.19	**0.003**	**0.015**	66.38	**0.004**	**0.018**	65.81	**0.004**	**0.032**	47.63	0.405	0.607
V3D	66.88	**0.008**	**0.024**	58.5	0.114	0.171	63.69	**0.039**	0.087	46.75	0.22	0.607
V3V	55.56	0.183	0.205	56.94	**0.015**	**0.044**	53.13	0.539	0.808	53.69	0.358	0.607
V3A	56.75	0.176	0.205	61.5	0.079	0.142	50.38	0.921	0.921	51.31	0.508	0.644
V7	56.94	**0.015**	**0.035**	45.44	0.259	0.333	49.69	0.915	0.921	50.25	0.901	0.901
VIPS	49.94	0.986	0.986	54.69	0.312	0.351	50.88	0.74	0.921	46.56	0.328	0.607
POIPS	58.19	**0.034**	0.05	59.44	**0.027**	0.061	53.5	0.127	0.229	52.31	0.392	0.607
DIPS	57.31	**0.032**	0.05	52	0.608	0.608	59	**0.009**	**0.041**	54.19	0.176	0.607

Table A.19: MVPA results of the Action phase in research topic 2#

ROIs	DG			AG			NG			UG		
	Accuracy (%)	**p**	**q**	**Accuracy (%)**	**p**	**q**	**Accuracy (%)**	**p**	**q**	**Accuracy (%)**	**p**	**q**
V1	71.5	**9E-04**	**0.008**	65.94	**0.004**	**0.011**	59.13	**0.031**	0.139	55.94	0.155	0.199
V2	67.5	**0.013**	**0.023**	70.56	**2E-04**	**0.001**	59.56	0.074	0.167	56.88	0.081	0.145
V3D	66	**0.008**	**0.023**	61.13	**0.046**	0.069	56.44	0.261	0.293	62.31	**8E-04**	**0.007**
V3V	60.69	0.088	0.098	66.31	**2E-05**	**2E-04**	55.69	0.256	0.293	60.94	**0.009**	**0.039**
V3A	59.19	0.109	0.109	61.56	**0.014**	**0.032**	56.38	0.192	0.288	58.38	0.054	0.121
V7	60.75	**0.037**	**0.047**	54.56	0.438	0.438	55.31	0.102	0.184	61	**0.04**	0.121
VIPS	59.75	**0.02**	**0.029**	58.31	0.094	0.105	55.94	0.061	0.167	53	0.359	0.359
POIPS	63.19	**0.009**	**0.023**	57.5	0.082	0.105	56.81	**0.018**	0.139	56.06	0.148	0.199
DIPS	61.25	**0.013**	**0.023**	58.88	**0.045**	0.069	52.88	0.4	0.4	54.63	0.332	0.359

Table A.20: MVPA results of the Judgement phase in research topic 2#

ROIs	DG			AG			NG			UG		
	Accuracy (%)	**p**	**q**	**Accuracy (%)**	**p**	**q**	**Accuracy (%)**	**p**	**q**	**Accuracy (%)**	**p**	**q**
V1	63.25	**0.016**	0.07	66.81	**5E-05**	**5E-04**	66.69	**0.002**	**0.017**	59.75	**0.011**	**0.034**
V2	65.56	**0.01**	0.07	67.06	**0.004**	**0.013**	62.75	**0.042**	0.094	65.06	**0.008**	**0.034**
V3D	59.81	0.094	0.169	64.31	**0.004**	**0.013**	62	**0.017**	0.075	60.19	**0.018**	**0.04**
V3V	56.88	0.075	0.168	58.38	0.064	0.082	57.56	**0.026**	0.077	65.44	**3E-04**	**0.003**
V3A	53	0.441	0.484	58.75	**0.02**	**0.044**	55.88	0.207	0.311	57.38	**0.046**	0.083
V7	57.13	0.074	0.168	55.69	0.13	0.139	47.06	0.482	0.482	52.31	0.612	0.688
VIPS	52.94	0.348	0.484	59.69	**0.035**	0.055	54.19	0.348	0.447	51.88	0.563	0.688
POIPS	52.75	0.484	0.484	57.5	**0.037**	0.055	56.31	0.114	0.206	51.31	0.771	0.771
DIPS	52.38	0.448	0.484	56	0.139	0.139	52.56	0.427	0.481	54.06	0.346	0.519

Table A.21: MVPA results of transfer-type classification from the Instruction phase in research topic 2#

ROIs	DG & UG			AG & UG			NG & UG		
	Accuracy (%)	**p**	**q**	**Accuracy (%)**	**p**	**q**	**Accuracy (%)**	**p**	**q**
V1	51.78	0.571	ns	49.56	0.876	ns	50.5	0.831	0.936
V2	49.59	0.907	ns	49.97	0.992	ns	49.66	0.912	0.936
V3D	52.91	0.388	ns	55.38	0.05	ns	55.84	**0.005**	0.072
V3V	52.22	0.306	ns	49.59	0.834	ns	52.19	0.109	0.575
V3A	53.5	0.083	ns	49.59	0.848	ns	50	1	0.936
V7	53.13	0.197	ns	49.81	0.929	ns	51.97	0.441	0.717
VIPS	48.75	0.57	ns	48.53	0.611	ns	46.59	0.057	0.254
POIPS	54.63	0.097	ns	49.5	0.857	ns	51.16	0.414	0.781
DIPS	47.63	0.309	ns	50.81	0.71	ns	48.53	0.351	0.717

Table A.22: MVPA results of transfer-type classification from the Action phase in research topic 2# used in Figure 3.4B

ROIs	DG & AG			DG & UG			AG & UG		
	Accuracy (%)	**p**	**q**	**Accuracy (%)**	**p**	**q**	**Accuracy (%)**	**p**	**q**
V1	58.72	0.065	0.085	56.78	0.089	0.115	53.25	0.142	0.475
V2	61.53	**0.015**	0.064	61.72	**0.005**	**0.03**	51.75	0.619	0.696
V3D	62.09	**0.014**	0.064	53.31	0.314	0.314	50.66	0.865	0.865
V3V	56.94	**0.046**	0.083	60.84	**0.009**	**0.03**	52.78	0.47	0.696
V3A	60.78	**0.029**	0.064	55.94	**0.034**	0.061	52.13	0.501	0.696
V7	57.31	0.066	0.085	54.22	0.123	0.138	54.28	0.17	0.475
VIPS	55.41	0.189	0.189	58.91	**0.01**	**0.03**	51.09	0.545	0.696
POIPS	60.22	**0.027**	0.064	55.78	0.061	0.092	52.88	0.211	0.475
DIPS	58.72	0.077	0.086	58.91	**0.02**	**0.046**	56.16	0.178	0.475

Table A.23: MVPA results of transfer-type classification from the Action phase in research topic 2# used in Figure 3.4C

ROIs	DG & NG			AG & NG			UG & NG		
	Accuracy (%)	**p**	**q**	**Accuracy (%)**	**p**	**q**	**Accuracy (%)**	**p**	**q**
V1	51.97	0.352	0.634	55.38	0.087	0.197	45.94	0.103	0.536
V2	53.81	0.1	0.299	57.97	**0.001**	**0.009**	47.75	0.45	0.579
V3D	59.13	0.076	0.299	56.5	0.086	0.197	46.56	0.276	0.536
V3V	47.59	0.347	0.634	54.09	0.183	0.235	47.97	0.357	0.536
V3A	50.94	0.718	0.807	56	0.077	0.197	45.81	0.167	0.536
V7	50.28	0.895	0.895	53.34	0.241	0.247	49.63	0.903	0.903
VIPS	51.53	0.636	0.807	53	0.247	0.247	52.22	0.287	0.536
POIPS	48.16	0.436	0.655	53.63	0.18	0.235	51.09	0.626	0.704
DIPS	46.75	0.054	0.299	46.22	0.149	0.235	48.72	0.348	0.536

Table A.24: MVPA results of transfer-type classification from the Judgment phase in research topic 2# (1 of 2)

ROIs	DG & AG			DG & NG			DG & UG		
	Accuracy (%)	**p**	**q**	**Accuracy (%)**	**p**	**q**	**Accuracy (%)**	**p**	**q**
V1	62.34	**0.005**	**0.016**	60.41	**0.036**	0.108	57.81	0.086	0.155
V2	65.38	**0.001**	**0.009**	63.28	**0.028**	0.108	63.66	**0.017**	0.079
V3D	65.16	**0.005**	**0.016**	55.97	0.248	0.447	60.13	**0.034**	0.101
V3V	56.66	0.059	0.089	54.75	0.1	0.225	54.31	0.062	0.139
V3A	56.44	**0.022**	**0.046**	56.69	**0.026**	0.108	57.63	**0.017**	0.079
V7	50.41	0.891	0.891	49.03	0.679	0.787	50.63	0.847	0.847
VIPS	54.88	**0.026**	**0.046**	49.47	0.807	0.807	52.5	0.411	0.529
POIPS	51.44	0.455	0.512	48.81	0.516	0.775	53.13	0.113	0.169
DIPS	47.13	0.274	0.352	50.78	0.699	0.787	52	0.509	0.573

Table A.25: MVPA results of transfer-type classification from the Judgment phase in research topic 2# (2 of 2)

ROIs	AG & NG			AG & UG			NG & UG		
	Accuracy (%)	**p**	**q**	**Accuracy (%)**	**p**	**q**	**Accuracy (%)**	**p**	**q**
V1	60.72	**0.02**	0.065	63.19	**0.002**	**0.017**	58.34	**0.013**	**0.038**
V2	64.5	**0.014**	0.065	64.28	**0.004**	**0.018**	59.63	**0.012**	**0.038**
V3D	61.13	**0.022**	0.065	57.94	0.051	0.114	59.88	**0.004**	**0.033**
V3V	59.25	**0.029**	0.066	58.06	**0.013**	**0.039**	54.22	0.188	0.339
V3A	54.81	0.124	0.224	52.91	0.248	0.446	54.97	**0.034**	0.076
V7	48.69	0.724	0.896	49.5	0.852	0.955	51.22	0.646	0.727
VIPS	49.28	0.851	0.896	49.16	0.642	0.955	50.25	0.923	0.923
POIPS	49.09	0.638	0.896	50.28	0.925	0.955	51.91	0.36	0.463
DIPS	49.69	0.896	0.896	49.88	0.955	0.955	53.03	0.255	0.383

Table A.26: MVPA results of transfer-type classification across phase between Instruction and Action phase in research topic 2# (1 of 2)

ROIs	DG			AG		
	Accuracy (%)	**p**	**q**	**Accuracy (%)**	**p**	**q**
V1	34.69	**0.004**	**0.023**	35.06	**8E-04**	**0.004**
V2	40.28	**0.005**	**0.023**	36.16	**0.006**	0.017
V3D	37.19	**0.008**	**0.023**	37.91	**0.018**	**0.04**
V3V	43.31	0.053	0.095	43.56	**2E-04**	**0.002**
V3A	41.56	**0.039**	0.087	44.03	**0.029**	0.052
V7	45.09	0.082	0.124	48.5	0.61	0.61
VIPS	47.84	0.384	0.384	45.44	0.197	0.254
POIPS	42.38	0.097	0.124	45.97	0.3	0.337
DIPS	44.56	0.199	0.224	42.94	0.068	0.101

Table A.27: MVPA results of transfer-type classification across phase between Instruction and Action phase in research topic 2# (2 of 2)

ROIs	NG			UG		
	Accuracy (%)	**p**	**q**	**Accuracy (%)**	**p**	**q**
V1	40.16	**0.031**	0.092	50.72	0.664	ns
V2	36.28	**0.003**	**0.013**	49.81	0.927	ns
V3D	32.63	**8E-04**	**0.007**	46.91	0.334	ns
V3V	41.5	**0.043**	0.097	46.31	0.117	ns
V3A	45.44	0.304	0.547	50.75	0.741	ns
V7	49.38	0.795	0.842	48.09	0.416	ns
VIPS	48.84	0.681	0.842	48.47	0.524	ns
POIPS	50.38	0.842	0.842	51.72	0.489	ns
DIPS	49.41	0.828	0.842	47.38	0.443	ns

List of publications and conferences

1. Peered review journals article (2)

1.1. Threethipthikoon T., Li Z., Shigemasu H. (2023). Orientation Representation in Human Visual Cortices: Contributions of Non-Visual Information and Action-Related Process, Frontiers in Psychology Volume 14 - 2023, Section Perception Science, DOI: 10.3389/fpsyg.2023.1231109, Accepted for publication. This journal included in WOS, IF: 4.232, Q1

1.2. Threethipthikoon T., Li Z., Shigemasu H. (2024). Orientation representation of visually occluded action in human visual cortices, submitted to Frontiers in Psychology, This journal included in WOS, IF: 4.232, Q1

2. International conference (2)

2.1. Threethipthikoon T., Li Z., Shigemasu H., Visually occluded grasp modulates orientation representation in human early visual cortex. in Poster session Perception & Action: Grasping, Vision Science Society (VSS 2023), at St. Pete Beach, Florida. May 23, 2023.

2.2. Threethipthikoon T., Li Z., Shigemasu H., Orientation representation for visually occluded action in V3d. Virtual Poster presentation, in V-VSS Poster Session 3, Virtual-Vision Science Society (V-VSS 2022), June 2, 2022.

3. International conference before doctoral program (2)

3.1. Threethipthikoon T., Li Z., Shigemasu H., Generalized Representation of 3D Object related to action in visual cortex: an fMRI Study. Poster presentation, International Workshop on Human-Engaged Computing (IWHEC 2019) at Kochi University of Technology. January 12, 2019.

3.2. Threethipthikoon T., Li Z., Shigemasu H., Generalized Representation of 3D Object Orientation in Human Visual Cortex. Poster presentation, Asia-Pacific Conference on Vision (APCV 2019), at Osaka, Japan. July 29 – August 1, 2019

Acknowledgment

Over the past four and a half years, my life has been a journey filled with both challenges and triumphs. From the moment I committed to pursuing a doctoral degree, I understood the formidable obstacles that lay ahead. Unexpected trials, such as abrupt shifts in research focus and the disruptive impact of the global pandemic, only served to amplify the complexity of this journey. What I encountered proved to be far more demanding than I initially anticipated, exponentially so. The experiences I gained along this path are invaluable and unmatched, impossible to replicate elsewhere. I am deeply grateful to the many individuals who supported, encouraged, and enriched my life throughout this journey.

First and foremost, I extend my heartfelt gratitude to my supervisor, Professor Hiroaki Shigemasu. During my master's degree, he played a pivotal role in deepening my understanding of research principles. Throughout my doctoral journey, he provided unwavering support, empowering me to unlock my potential in seeking answers and drawing independent conclusions. Despite moments when I couldn't fully devote myself to my studies, Professor Shigemasu's kindness and patience never faltered. He remained steadfast in his support, guiding me through the challenges until I successfully completed my journey.

I am equally thankful to my co-supervisors, Professor Hiroshi Kadota and Professor Kiyoshi Nakahara, whose insightful perspectives and constructive feedback illuminated new pathways in my study. My gratitude also extends to the esteemed members of my dissertation committee, Professor Keizo Shinomori and Professor Yukinobu Hoshino, for their meticulous review and invaluable contributions.

Special appreciation goes to Dr. Zhen Li, my senior colleague in the laboratory, for providing invaluable technical support throughout the data analysis process and offering valuable insights into the paper submission process. Additionally, I am deeply thankful to all the participants of my fMRI experiments, whose generosity in dedicating their time and energy to long sessions proved instrumental to my research.

To my Thai friends at KUT, I am grateful for the invaluable experiences we shared and for ensuring that I never felt alone during the challenges of the PhD journey. Similarly, I extend my appreciation to Dr. Bandhit Suksiri, whose unwavering support has been a constant source of strength since my master's degree and continues to be precious to me to this day.

I express my heartfelt appreciation to my family in Thailand for their unwavering understanding and support, for which I am forever grateful. Additionally, I am deeply

thankful to my girlfriend for her understanding of my circumstances and for providing invaluable emotional support, despite our recent acquaintance.

Lastly, I want to express my gratitude to Porter Robinson for his songs "Something Comforting" and "Look at the Sky," which have been sources of consolation and inspiration during difficult times.

Thanaphop Threethipthikoon

March 2024